Application of percolation threshold to disintegration and dissolution of ibuprofen tablets with different microcrystalline cellulose grades

Ana Luiza P. Queiroz[1], Barbara Wood[2,3], Waleed Faisal[1,4], Fatma Farag[1,4], Hazel Garvie-Cook[5], Brian Glennon[2], Sonja Vucen[1], Abina M. Crean*[1]

[1] *SSPC Pharmaceutical Research Centre, School of Pharmacy, University College Cork, Cork, Ireland*

[2] *SSPC Pharmaceutical Research Centre, School of Chemical and Bioprocess Engineering, University College Dublin, Dublin 4, Ireland*

[3] *APC Ltd, Cherrywood Business Park, Loughlinstown, Co Dublin, Ireland*

[4] *School of Pharmacy, Minia University, Al Minyā, Egypt*

[5] *Renishaw plc, New Mills, Wotton-under-Edge, Gloucestershire, GL12 8JR, UK*

*Corresponding Author.

Tel: + 353 (21) 4901667

Email: a.crean@ucc.ie

ABSTRACT

This study investigated whether a step change in disintegration and dissolution behaviour was observed for tablets prepared below and above a percolation threshold. The percolation threshold investigated was previously calculated for ibuprofen/ microcrystalline cellulose (MCC) blends using percolation theory and compression data (Queiroz et al., 2019). The influence of MCC grade (air stream dried versus spray dried) on differences observed was also studied. Complementary to conventional disintegration and dissolution testing, Raman imaging determined drug distribution within tablets, and in-line particle video microscopy (PVM) and focused-beam reflectance measurement (FBRM) monitored tablet disintegration. Tablets were prepared containing 0 to 30% w/w ibuprofen. Raman imaging confirmed the percolation threshold by quantifying the number and equivalent circular diameters of ibuprofen domains on tablet surfaces. Across the percolation threshold a step change in dissolution behaviour occurred and tablets containing air stream dried MCC showed slower disintegration and dissolution compared to tablets containing spray dried MCC. Dissolution measurements confirmed experimentally a percolation threshold, determined using percolation theory and compression data. An increase in drug domains, due to cluster formation, and less efficient tablet disintegration contributed to slower ibuprofen release above the percolation threshold. Slower dissolution was measured for tablets containing air stream dried compared to spray dried MCC.

1. INTRODUCTION

Disintegration and dissolution profiles are critical quality attributes assessed to evaluate drug release performance (Dressman and Krämer, 2005; Huang et al., 2011; Nickerson et al., 2018). Disintegration is often the rate determining step for drug release, particularly for poorly water soluble drugs (Caramella et al., 1988). Disintegration is the mechanical fragmentation of the compressed tablet into small granules or agglomerates. Disintegration is initiated by liquid penetration in the porous of the compact. Swelling is one of the most accepted disintegration mechanisms, which is characterized by an enlargement of the particles that builds up pressure to fragment the tablet matrix (Markl and Zeitler, 2017). The bonding mechanism during compression and the bonding surface area have a direct impact on tablet disintegration. Swelling depends on an optimal tablet porosity, such that the liquid can enter the tablet matrix, however, the void spaces are too large enough to supress the swelling action of disintegrants (Desai et al., 2016).

The application of modelling approaches to enhance product knowledge has been motivated by quality guidelines as an alternative to iterative testing approaches during formulation development (International Council for Harmonisation, 2012, 2008, 2005a, 2005b; Kimura et al., 2013). The percolation threshold model has been used to explain how particle-particle interactions of drug and diluents alters dissolution performance of formulations containing different drug loadings (Bonny and Leuenberger, 1993, 1991). In this context, the percolation threshold is the drug loading in which clusters of the drug span throughout the entire volume of the tablet, i.e. an infinite cluster is formed. When this cluster is formed properties of the blend may undergo significant changes (Leuenberger, 1999).

Previous studies determined the percolation threshold value from disintegration and dissolution experimental data (Kimura et al., 2007a; Stillhart et al., 2017; Wenzel et al., 2017). These studies experimentally determined critical loadings at which disintegration times undergo a step change. These were then assumed to be the percolation thresholds. However, Kimura, Betz and Leuenberger, 2007 recommended further studies to investigate if the change in disintegration behaviour was linked to the formation of the infinite cluster described by the percolation threshold theory (Kimura et al., 2007b). Since these earlier studies, technological advancements have provided novel techniques to study drug distribution in tablets and tablet disintegration behaviour. These techniques can be key to providing data to support the percolation threshold concepts and the findings of previous studies.

Spectral imaging techniques have been used to provide in depth information related to drug distribution in pharmaceutical tablets. These techniques can be used to investigate the cluster formation predicted by the percolation theory. Fourier transform infrared spectroscopy (ATR-FTIR), X-ray diffraction (XRD), and Raman spectroscopy are the main techniques employed (Chan et al., 2005; Kazarian and Ewing, 2013; Miller and Havrilla, 2005; Zhang et al., 2005). Among those, advancements in Raman instruments has enabled the technique to rapidly map drug distribution in tablets. Raman imaging instruments have been designed to capture rich spectroscopic data which can be translated to provide high-resolution chemical information for tablets (as low as 1 µm per pixel) and require short acquisition times (approx. 15 min for a tablet of 13 mm diameter) (Ali et al., 2013).

Focused Beam Reflectance Method (FBRM) and in-line Particle Video Microscopy (PVM) are innovative techniques that can give real-time in-situ information regarding disintegration and dissolution performance of tablets. FBRM has been used to monitor the rate and the

85 degree of change in the number of particles and particle structures in a process (Barrett et
86 al., 2011; Gregory, 2009; Simon et al., 2019; Zhong et al., 2020). Measurement of the solid
87 particles using FBRM is performed without the need for sampling and performing off-line
88 analysis. The system gives particle count, dimension and shape information in real time by
89 monitoring changes in the system as they occur (Barrett and Glennon, 1999). PVM provides
90 real-time images of the system allowing the user to visually track changes in the solids over
91 time (Barrett and Glennon, 2002). The imaging window measures an area of approximately
92 800 µm by 1100 µm. PVM also records a Relative Backscatter Index (RBI) trend which can be
93 used to track changes in the shape and size of solid particles as well as changes in the solids
94 concentration (Werner et al., 2017). RBI is comparable to turbidity monitoring. Increased
95 RBI indicates a larger amount of solids (Hartwig and Hass, 2018). As tablet disintegration
96 progresses the number of particles in the slurry increase as larger particles fragment.
97 Therefore, as disintegration proceeds, more particles are captured in the image and the RBI
98 increases.
99 FBRM and PVM techniques are commonly used in crystallization studies (mass transfer from
100 solution to solid phase) (Barrett et al., 2011; Hartwig and Hass, 2018; Jiang et al., 2014; Liu
101 et al., 2011; Mitchell et al., 2011; Simon et al., 2019; Simone et al., 2015). FBRM has also
102 been utilized in previous studies for investigating tablet disintegration and dissolution
103 (Coutant et al., 2010; Han et al., 2009; Menning, 2016; Metzler et al., 2017). PVM has the
104 potential to monitor tablet disintegration and dissolution because changes in particle size
105 and shape in suspension are key features observed during tablet disintegration and
106 dissolution.
107 The aim of this study was to investigate if a step change in disintegration and dissolution
108 behaviour was observed for tablets produced with drug loadings below and above a

predetermined percolation threshold. The percolation threshold of these systems was determined in an earlier study using the physical principals of blending and compaction (Queiroz et al., 2019). The model system investigated was tablets produced from binary blends of microcrystalline cellulose (MCC) and ibuprofen (IBU) at a range of ibuprofen mass loadings. Tablets were prepared with two different MCC grades; one spray dried and one air stream dried. The percolation threshold values determined were 19.08% w/w and 17.76% w/w IBU for blends with air stream dried MCC and spray dried MCC, respectively (Queiroz et al., 2019). A secondary study aim was to determine if the grade of MCC altered any changes in disintegration and dissolution behaviour observed.

In the context of the previous and the present study, percolation threshold is a geometric phase transition in which the concentration of ibuprofen particles is high enough to form a cluster that spans throughout the entire volume of the tablet. When this ibuprofen particle cluster is formed, it is anticipated that a step change in properties of the blend will occur. For example, a reduction in flow, compaction and dissolution would be anticipated with ibuprofen particle cluster formation, as ibuprofen has poor flowability and compressibility properties compared to MCC (Al-Karawi et al., 2018; Liu et al., 2008), and is considerably more hydrophobic (Kawabata et al., 2011).

In addition to traditional pharmacopeial disintegration and dissolution techniques, process analytical technologies (PAT) FBRM and PVM were employed to better understand tablet disintegration behaviour, and hence its influence on drug dissolution. Building on the application of Raman imaging to qualitatively identity clusters of ibuprofen particles (Queiroz et al., 2019), the present study demonstrated how Raman spectroscopy can be used to quantitatively determine the size and the number of ibuprofen clusters formed on tablets surfaces and hence confirm the percolation threshold determined from compaction

133 data. The MCC grades studied, have similar specifications; average particle size of 130 µm
134 and similar bulk density (0.28 - 0.33 g/mL for the air stream dried and 0.25 – 0.37 g/mL for
135 the spray dried). In the earlier study, Queiroz et al., reported morphological differences
136 between both grades: air stream dried showed bigger particles with needle shaped
137 geometry, while spray dried showed smaller particles with a more spherical-shaped
138 geometry (Queiroz et al., 2019).
139

140 **2. MATERIALS**

141 Emcocel®90 (spray dried) and Vivapur®102 (air stream dried) were supplied by JRS Pharma
142 (Weissenborn, Germany) and ibuprofen by Kemprotec (Cumbria, UK). The two MCC
143 products studied were medium size standard grades with theoretical bulk density of 0.28 -
144 0.33 g/mL for the air stream dried and 0.25 – 0.37 g/mL for the spray dried MCC. A range of
145 particulate and bulk powder properties of the batches of ibuprofen, air stream dried MCC
146 and spray dried MCC used in this study had been previously determined (Table 1) (Queiroz
147 et al., 2019). Other materials used such as buffer components and HPLC mobile phase were
148 all supplied by Sigma Aldrich, Ireland.

149 Table 1. Particulate and bulk powder properties of Air stream dried®, Spray dried MCC®, and
150 ibuprofen. Average values are shown ± standard deviation (Queiroz et al., 2019).

Property	Spray dried MCC®	Air stream dried®	Ibuprofen
D10 (µm) (n=5)	30.0 ± 0.25	31.1 ± 0.30	16.5 ± 0.08
D50 (µm) (n=5)	111.6 ± 0.73	118.0 ± 1.60	54.9 ± 0.21
D90 (µm) (n=5)	236.8 ± 1.55	240.0 ± 2.17	129.0 ± 1.09
Surface area (m^2/g) (n=3)	1.32 ± 0.01	1.37 ± 0.01	0.22 ± 0.02
True density (g/cm^3) (n=10)	1.58 ± 0.00	1.57± 0.00	1.12 ± 0.00
Bulk density (g/cm^3) (n=3)	0.33 ± 0.00	0.31 ± 0.00	0.36 ± 0.01

Relative density	0.21	0.20	0.32
Tapped density (g/cm^3) (n=3)	0.43 ± 0.01	0.40 ± 0.00	0.57± 0.01
Hausner Ratio	1.32 (easy flowing)	1.32 (easy flowing)	1.58 (cohesive)
Flow function coefficient (n=3)	7.0 ± 0.91 (easy flowing)	6.9 ± 0.00 (easy flowing)	3.9 ± 0.11 (cohesive)

3. METHODS

3.1 Tablet manufacture and characterization

Binary blends of MCC and IBU were prepared containing a range of IBU concentrations: 2.5, 5, 7.5, 10, 12.5, 15, 20, and 30 % w/w. Each blend, total weight 300 g, was prepared using a cube mixer KB 15 (Erweka, Heusenstamm, Germany) at 30 rpm for a duration of 30 min. Flat, round, 8 mm tablets were manufactured using a 10 punches Piccola rotary tablet press (Riva, Buenos Aires, Argentina) rotating at 20 rpm. The tablet hardness was controlled to 120 ± 10 N, tablet weight variation to 270 ± 10 mg, and the room air humidity to 50 ± 5 % and temperature to 19 ± 2 °C.

Tablet porosity was determined using Equation 1. Tablet envelope density was determined dividing the mass by the volume of each tablet. The blend true density values were previously determined (Queiroz et al., 2019).

$$Porosity = 100 \times \left[1 - \left(\frac{tablet\ envelope\ density}{blend\ true\ density}\right)\right] \quad \text{(Equation 1)}$$

3.2 Raman imaging analysis of tablet surface

Drug and excipient distributions on external surfaces and surfaces of internal sections of tablets were investigated by Raman imaging analysis using a RA802 Pharmaceutical analyser

(Renishaw, New Mills, UK). First, reference spectra of air stream dried MCC, spray dried MCC, and ibuprofen were acquired. Then, tablets of the blends of ibuprofen and MCC were screened using the StreamLineTM fast imaging method that acquired around 76,000 spectra over the entire surface of each tablet, with a pixel size of 10um/20um, and those spectra were averaged to a single resulting spectrum. The total time of measurement for each individual tablet was 15 min. Images of the drug distribution on the surface of the tablet were generated by non-negative least squares (NNLS) component analysis. Domains of each substance were determined based on the reference spectra acquired for the pure substances. Domains of each substance in the generated images were analysed using Particle Analysis in Renishaw's WiRE software. This software resolves the image domains and determines particle metrics. The numbers of domains of ibuprofen on the entire surface of each tablet and their average equivalent circle diameters were determined.

Principal component analysis (PCA) was performed using the average spectra obtained from Raman imaging analysis. Unscrambler X (Camo Analytics, Oslo, Norway) was used to perform the PCA with full cross validation, using the algorithm Singular Value Decomposition (SVN).

3.3 Disintegration analysis

In vitro disintegration time was determined in water at 37 °C ± 2 °C, using a tablet disintegration tester ZT42 (Erweka, Edison, USA) which complies with Ph. Eur. 2.9.1 (Disintegration of tablets and capsules) (Council of Europe, 2019). Each tablet was placed inside of one basket which were continuously and automatically agitated vertically in the disintegration medium. The disintegration process was observed until the tablets

disintegrated into small enough particles that could escape the basket so that no substantial material remained in the basket. Analysis was performed in triplicate.

3.4 FBRM and PVM analysis

FBRM (FBRM G600) and PVM (PVM V19) (Mettler Toledo, Leicester, England) were used to monitor tablet disintegration using a Mettler Toledo Easymax^{TM} 102 system. The disintegration medium was phosphate buffer (pH 7.2). The system used consisted of 100 mL glass vessels with automated internal temperature and agitation control. System specific PTFE (polytetrafluoroethylene) lids allowed for integration of the FBRM and PVM probes. A visual check of the system was possible through an inspection window at the front of the system.

The working volume of the system was 50 mL. Experiments were performed at 37 °C and the agitation rate was 250 rpm using an upward pumping, pitch blade impeller for a minimum of 10 minutes after the tablet was added to the vessel. The powder or tablet was added to the glass vessel under agitation. PVM and FBRM monitoring was performed throughout the duration of the experiment; FBRM data was recorded every 2 seconds and two PVM images were recorded every second.

3.5 Dissolution studies

The dissolution studies were carried out using a DT 600 dissolution tester of Ph. Eur. 2.9.3 (paddle) (Erweka, Edison, USA). A volume of 500 mL of phosphate buffer pH 7.2 equilibrated at 37 ˚C was used as the dissolution medium and the paddle rotation was kept at 50 rpm. Solubility of ibuprofen in the given conditions is 3.74 mg/ml (Dabbagh and Taghipour, 2007). The experiment was conducted using sink conditions; the theoretical concentration of Ibuprofen in the dissolution medium following complete dissolution of 30 % w/w ibuprofen

212 tablets was 0.16 mg/ml. Following addition of the tablet sample to the dissolution medium,
213 samples of 0.5 ml volume were withdrawn at 1, 5, 15, 30, 60 and 120, 180, and 240 min
214 intervals in order to determine the dissolution profiles. An additional sample was taken at
215 the 24 h time point to determine the total amount of drug in each tablet tested. At the 24 h
216 time point the tablet had completely disintegrated and complete IBU dissolution was
217 assumed.

218 All samples were filtered with 0.45 µm filter and 0.5 mL of fresh, pre-warmed medium was
219 immediately added to the system in order to correct the volume to the sample volume
220 withdrawn. Samples were analysed by HPLC. The % cumulative amount IBU released was
221 calculated and plotted against time.

222 HPLC analysis was performed using an Agilent 1200 series HPLC system with an UV/Vis
223 detector (Agilent Technologies, Santa Clara, USA). A reversed-phase column (Gemini C-18,
224 250 × 4 mm x 5 µm, Phenomenex Ltd. UK), mobile phase of acetronitrile and water (60:40,
225 pH adjusted to 2.5) at a flow rate of 1.5 ml/min and injection volume of 20 µL were
226 employed. The wavelength for Ibuprofen detection was set at 215 nm and retention time
227 was 7 min.

228 **4. RESULTS**

229 4.1 Tablet Characterisation

230 The average content of ibuprofen was determined for all tablets analysed and compared to
231 the theoretical content (Table 2). Greatest variance between actual and theoretical content
232 was measured for the 30 % w/w ibuprofen loading. Drug content uniformity was also
233 determined with the percentage relative standard deviation less than 7 % for all drug
234 loading. Tablet porosity was also determined (Table 2) as it can influence tablet

disintegration and dissolution (Ibrahim, 1985; Yassin et al., 2015). Porosity of tablets decreased as ibuprofen content increased. The porosity of tablets containing spray dried MCC was slightly greater than tablets containing the air stream dried MCC at all drug loadings except for 15%.

240 Table 2. Tablet ibuprofen theoretical and average actual content ± % relative standard deviation (n=5), blend true density and tablet porosity

Theoretical drug concentration (% w/w)	Theoretical drug content (mg)	Air stream dried MCC				Spray dried MCC			
		Actual drug content (mg)			Porosity (%)	Actual drug content (mg)			Porosity (%)
2.5 %	6.75	6.63	±	2.60 %	30.3	6.82	±	1.57 %	32.3
5 %	13.50	13.40	±	2.21 %	30.9	13.17	±	2.79 %	31.1
10 %	27.00	27.33	±	2.81 %	28.5	27.06	±	1.38 %	29.7
15 %	40.50	41.68	±	1.78 %	28.6	41.94	±	5.02 %	28.5
20 %	54.00	54.13	±	4.26 %	26.1	55.04	±	2.01 %	28.4
30 %	81.00	78.33	±	6.77 %	23.1	85.34	±	2.00 %	24.10

241

Commented [CA1]: New table with True Density of blends

242 4.2 Raman imaging analysis of tablet surface

243 Raman spectroscopy did not show differences between the characteristic bands of the MCC
244 tablets (air stream dried and spray dried MCC only), indicating similar chemical identity of
245 microcrystalline cellulose between grades. In respect to the ibuprofen loading, spectral
246 peaks related to ibuprofen increased in intensity when ibuprofen loading was increased
247 (Figure 1).

248 Raman images for tablets of all drug loadings were previously published (Queiroz et al.,
249 2019). In this study the number of ibuprofen domains on surfaces of each tablet was
250 determined from these Raman images, as described in section 3.2 The number of ibuprofen
251 domains decreases for the tablets with drug loading above 15 % w/w (Table 3), despite an
252 increase in the overall intensity peaks related to ibuprofen (Figure 1). Above the percolation
253 threshold the domains of ibuprofen start to connect to the neighbouring ibuprofen
254 domains. Thus, one single domain with larger area is counted, instead of numerous smaller
255 neighbouring domains. In the case of the compacted tablets, it results in a change in the
256 drug distribution from dispersion of drug particles in a matrix of MCC (large number of small
257 drug domains) to distribution of MCC in a matrix of drug (smaller number of larger drug
258 domains). The resulting larger domains where characterized by continuously increased
259 equivalent circular diameter of ibuprofen domains with a more pronounced increase
260 between the concentrations of 15% and 20% w/w ibuprofen (Table 3). These results build
261 on the results in the earlier study which qualitatively confirmed the percolation threshold
262 values determined by visual appearance, which can be subjective. In this study the
263 quantitative data obtained related to the number and size of ibuprofen domains provides a
264 less subjective confirmation of the percolation threshold value. It is important to consider

265 the presence of these larger clusters of drug as they can alter the tablet disintegration and

266 drug dissolution behaviour.

267

A

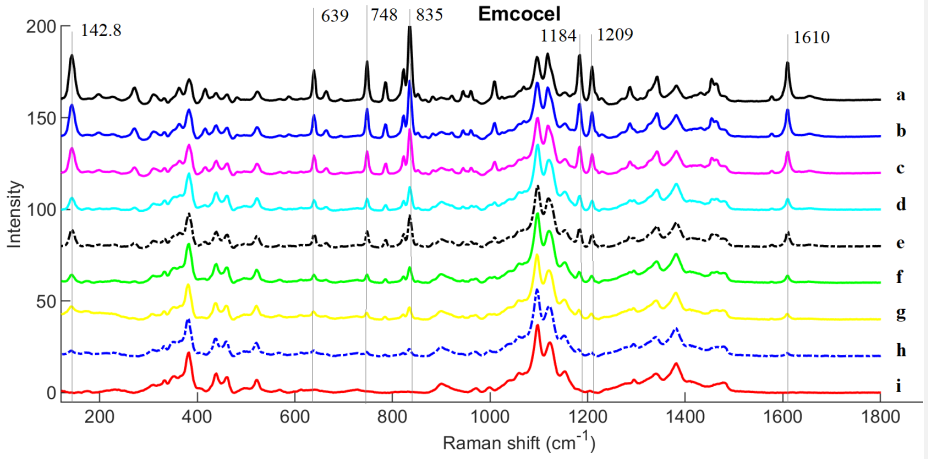

B

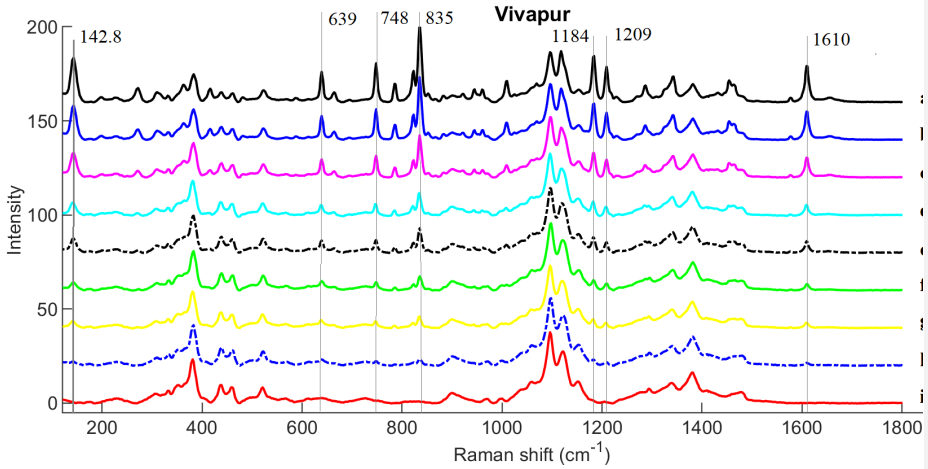

268 Figure 1. Average Raman spectra of the surface of (A) Spray dried MCC® and (B) Air stream

269 dried® tablets containing a range of ibuprofen loadings: (a) 30 %, (b) 20 %, (c) 15 %, (d) 12.5

%, (e) 10 %, (f) 7.5 %, (g) 5 %, (h) 2.5 %, and (i) 0 % ibuprofen w/w. Vertical lines indicate characteristic peaks of ibuprofen.

Table 3. The number of ibuprofen domains (N) and the equivalent circular diameter (ECD) of ibuprofen domains on the surface of Spray dried MCC® and Air stream dried® tablets containing a range of ibuprofen loadings (2.5 to 30% w/w ibuprofen). The number of domains (N) and the equivalent circular diameter values were determined from images generated using Raman image analysis.

% w/w Ibuprofen	Air stream dried®		Spray dried MCC®	
	N	ECD of ibuprofen domains (μm)	N	ECD of ibuprofen domains (μm)
2.5 %	158	69.2	130	62.0
5 %	264	70.4	218	59.6
7.5%	264	76.7	343	74.4
10 %	462	79.5	475	71.8
12.5%	377	74.3	469	77.1
15 %	513	90.5	483	88.6
20 %	377	103.5	376	103.4
30 %	112	153.7	72	138.9

PCA analysis of Raman spectra of the surface of tablets showed that the first principal component (PC-1) captured the effect of drug loading, while the second principal component (PC-2) captured variability within the samples due to both MCC grade and due to ibuprofen drug loading. The scores plot showed samples that are similar or different from each other, i.e. samples geometrically located at distance are dissimilar to each other while neighbouring samples are similar (Figure 2a). PC-1 and PC-2 explained 88% and 7% of the variance captured by the model, respectively. Raman shifts of 93, 142.8, 639, 748, 835, 1184, 1209, and 1610 cm^{-1} were the variables that mostly contributed to discriminate the samples along the first component of the model (PC-1) (Figure 2b). Those bands are

characteristic of ibuprofen (Sütő et al., 2016) and they were not observed in the spectra of the tablets containing pure MCC (Figure 1). As stated previously, these peak heights increased with the increase in drug loading. The PCA model showed that tablets containing air stream dried MCC differed from tablets containing spray dried MCC along PC-2. Loadings of PC-2 contained peaks assigned to both, ibuprofen and MCC. PC-2 also showed an upwards shifting of the baseline reduction in Raman shift. Both chemical and physical attributes of the tablets may explain this variability in Raman spectra. Differences in tablet porosity was observed with increase in drug loading and between MCC grades, Table 2. Raman spectra can show stronger intensities for samples for more compacted (less porous) samples due to an increased number of scattering molecules that will produce a Raman signal (https://doi.org/10.1016/j.vibspec.2018.10.011). The upwards shift may also be due to Raman fluorescence, which is a material-dependant phenomenon; fluorescence is phenomena intrinsic to MCC. Microcrystalline cellulose is known to be fluorescent mainly due to the presence of lignin (Castellan et al., 2007). Variance related to ibuprofen peaks (e.g. at the shifts 835 and 1610 cm^{-1}) and the main characteristic Raman bands assigned to cellulose (e.g. at 1096 cm^{-1} and within the region 275-550 cm^{-1}) (Wiley and Atalla, 1987) are also present in the loadings of PC-2. The region of 275-550 cm^{-1} is known to hold crystallinity information of cellulosic materials (Agarwal et al., 2010). Thus, the separation of the

Commented [CA2]: https://doi.org/10.1016/j.vibspec.2018.10.011
Gomez et al

306 samples along PC-2 may be an indication that the differences between the spray dried and

307 the air stream dried MCC grades included crystallinity, lignin content, and compact density.

308

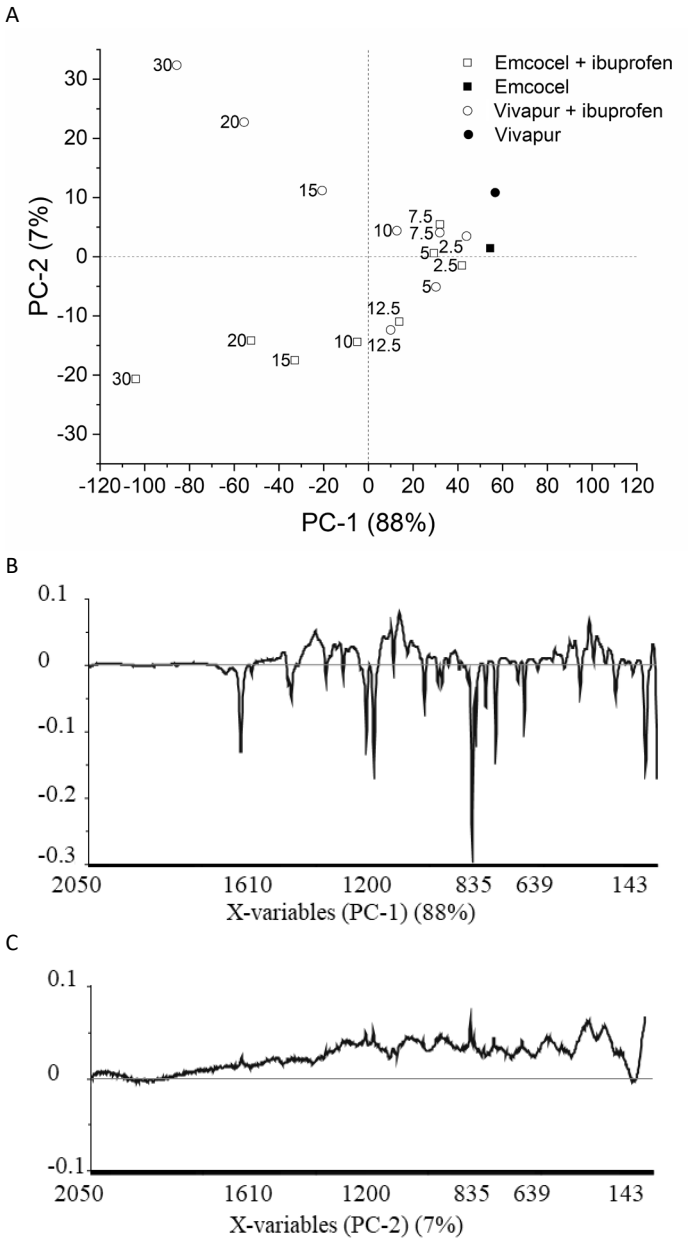

Figure 2 (A) Scores plot and (B and C) loading plots of the principal component analysis of Raman spectra acquired from spray dried MCC and air stream dried tablets and tablets containing a range of ibuprofen loadings (2.5 % to 30 % w/w ibuprofen). PC-1 and PC-2 are the first and the second principal components, respectively.

4.3 Disintegration and Dissolution

Tablet disintegration using Ph. Eur. 2.9.1 disintegration apparatus showed that all tablets had completely disintegrated in less than 5 min. Differences between tablets containing different drug loadings or MCC grades could not be accurately determined. The tablets investigated contain a high percentage in mass of MCC, which is highly hydroscopic and a noted disintegrant (Rowe et al., 2009). Thus, disintegration happened fast independently of the MCC grade.

The results of the Ph. Eur. 2.9.3 dissolution study showed that increased ibuprofen concentration had a negative impact on the dissolution behaviour of Ibuprofen/MCC tablets (Figure 3). The effect of ibuprofen loading on drug dissolution was evident for ibuprofen concentrations above the percolation threshold, 20 and 30 %w/w of ibuprofen; time to achieve 100% ibuprofen release increased significantly (Figure 4). Tablets containing the air stream dried MCC showed statistically significantly greater times to achieve 100% ibuprofen release for all drug loadings in comparison to tablets containing the spray dried MCC. Tablets containing 30% w/w IBU and air stream dried MCC did not reach %100 release in 240 min. Complete release was confirmed after 24h. It is also interesting to note the step change in time to reach 100% cumulative drug release between 2.5 and 5% drug loading (air stream dried MCC) and 2.5 and 7.5% drug loading (spray dried MCC respectively) (Figure 4). This change in dissolution behaviour is not related to a percolation threshold of ibuprofen in the MCC matrix but may be due to other factors such a differences in porosity influencing disintegration behaviour (Desai et al., 2016) and hence dissolution.

335

A

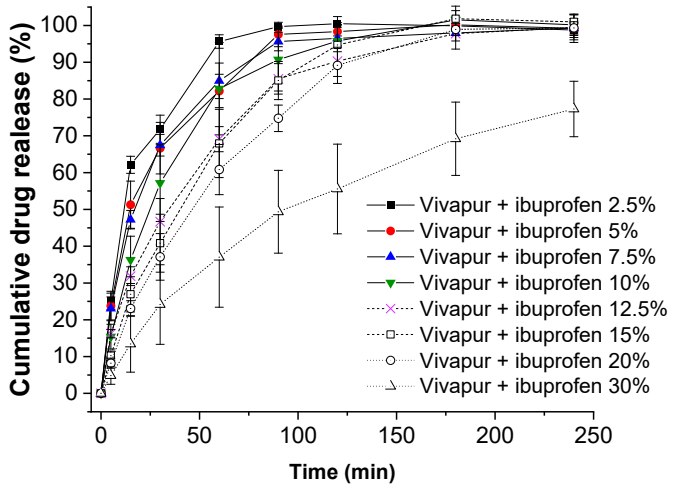

B

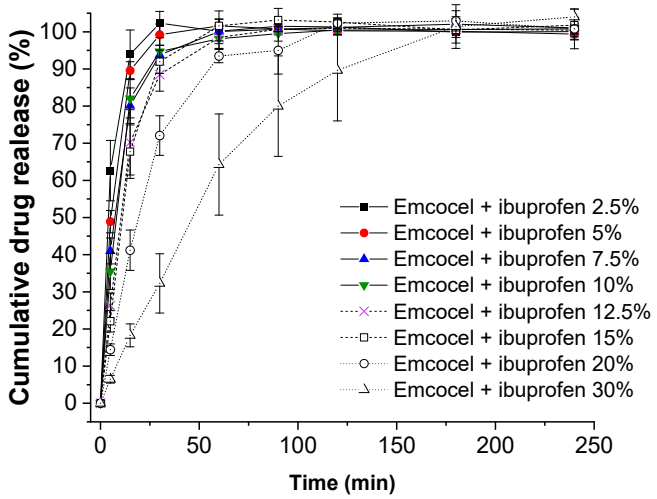

336 Figure 4. Dissolution profiles of tablets containing (A) Spray dried MCC® and (B) Air stream
337 dried® and different ibuprofen w/w/ loadings (2.5 to 30% w/w). Dissolution was performed
338 in phosphate buffer pH 7.2 at 37ºC. Average values shown with y-error bars indicating
339 standard deviation, n= 5.

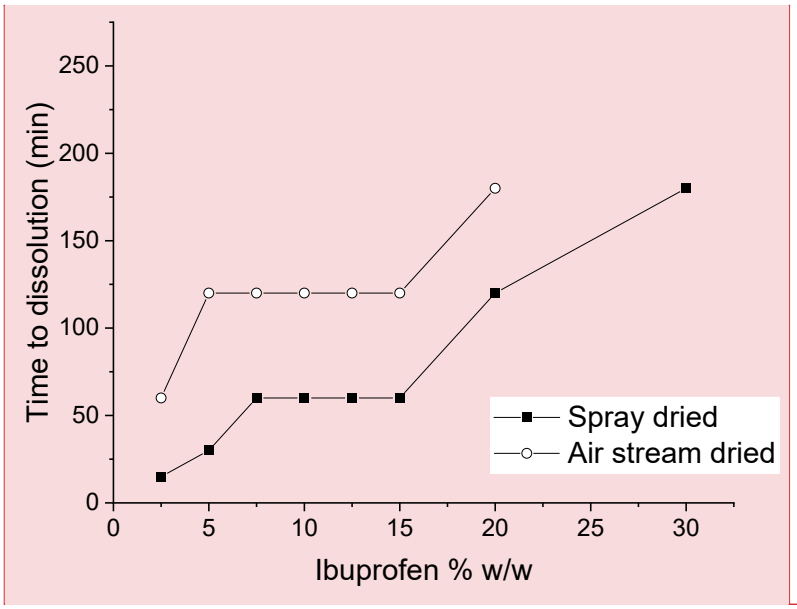

Commented [CA3]: Can you rescale Y axis to 200 min

Figure 4. Time to reach 100% ibuprofen release during dissolution of tablets containing spray dried and airs stream dried microcrystalline cellulose grades and different ibuprofen w/w/ loadings (2.5 to 30% w/w). Tablets containing air stream dried MCC and 30% w/w of ibuprofen did not reach %100 release in 240 min. However, complete release was confirmed after 24h. Dissolution was performed in phosphate buffer pH 7.2 at 37ºC. Average values shown with y-error bars indicating standard deviation, n= 5.

4.4 FBRM monitoring

FBRM was used as a PAT tool to determine if tablet disintegration played a role in the differences observed between dissolution of tablets containing air stream dried and spray dried MCC grades with increasing drug loading. Two aspects were investigated: the differences among tablets below and above the percolation threshold and the differences between both MCC grades. This analysis was complementary to the pharmacopoeial disintegration test which was not able to capture differences regarding these two aspects. As mentioned previously, FBRM gives particle count, dimension information in real-time

(Barrett and Glennon, 1999). It was hoped that the ibuprofen clusters observed in the tablets by Raman imaging could be observed in the disintegration medium and potentially explain the differences in dissolution observed between tablets containing spray dried and air stream dried MCC grades at different drug loadings.

Initially, disintegration monitored by FBRM was performed using spray dried and air stream dried MCC tablets without ibuprofen to determine differences in disintegration due to MCC grade. Both tablets displayed very similar behaviour with a sharp increase in particle counts upon addition of the tablet to the phosphate buffer pH 7.2. Figure 5 shows that the counts vs time profile for the two MCC grades were very similar, indicating that the tablets disintegrated at the same rate.

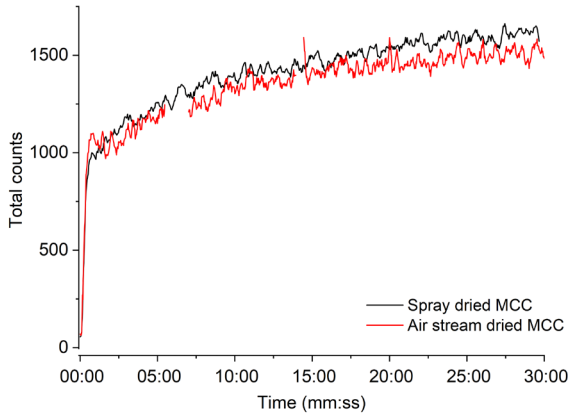

Figure 5. Focused Beam Reflectance Measurement (FBRM) counts 1-1000 µm versus time for tablets containing air stream dried and spray dried MCC in phosphate buffer pH 7.2, and temperature of 37 °C.

Figure 6 shows the FBRM total counts vs time for ibuprofen tablets added to the disintegration medium for the first 30 minutes. For all tablets there is a rapid increase in counts for the first 7 minutes approximately, indicating that, as with the tablets of air

stream dried and spray dried MCC without ibuprofen, tablet disintegration began immediately upon addition of the tablet to the medium for all ibuprofen loadings. A similar profile is seen for each tablet of spray dried MCC regardless of ibuprofen loading. The counts increased sharply in the first 30 seconds after addition to the medium and then continued to increase at a slower rate for the following minutes.

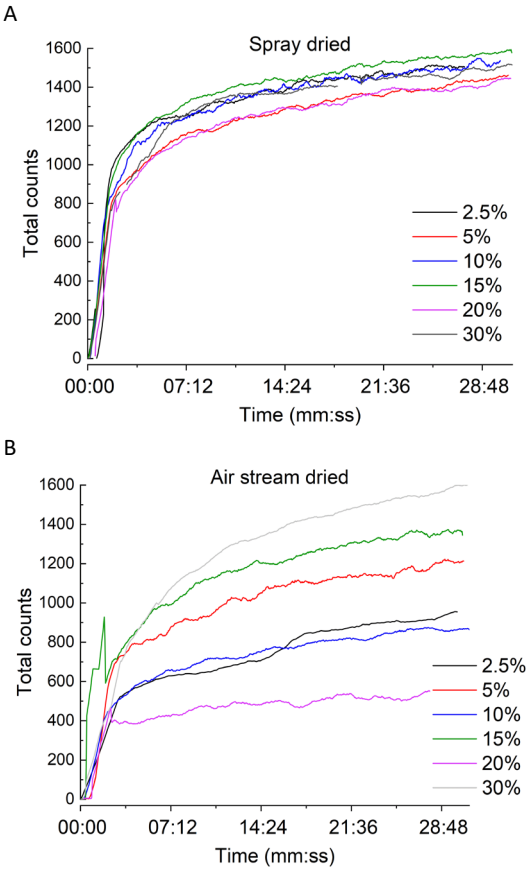

Figure 6. Focused Beam Reflectance Measurement (FBRM) total particle counts (counts 1-1000 µm) versus time for tablet containing (A) the spray dried MCC and (C) the air stream dried MCC and a range of ibuprofen loading (% w/w) in phosphate buffer pH 7.2 and temperature of 37 °C.

385 Overall, air stream dried MCC tablets had a much less consistent total counts profile over
386 time for different drug loading, in comparison to spray dried MCC tablets. When the
387 different ibuprofen loadings were compared, the loadings of 20 % and 30 % w/w ibuprofen
388 showed different profiles compared to lower drug loadings. For 20 % and 30 % w/w
389 ibuprofen, a sharp increase in total counts was observed upon addition of tablet and
390 followed by a rapid decrease. For tablets of air stream dried MCC at greater ibuprofen
391 loadings the total count was lower after 5 minutes compared to lower tablet loadings.

392 The total counts profiles for tablets containing air stream dried MCC was also lower in
393 comparison to tablets containing spray dried MCC, for all ibuprofen loadings (Figure 7).
394 These differences were more pronounced above the percolation threshold > 15% ibuprofen.

395

396

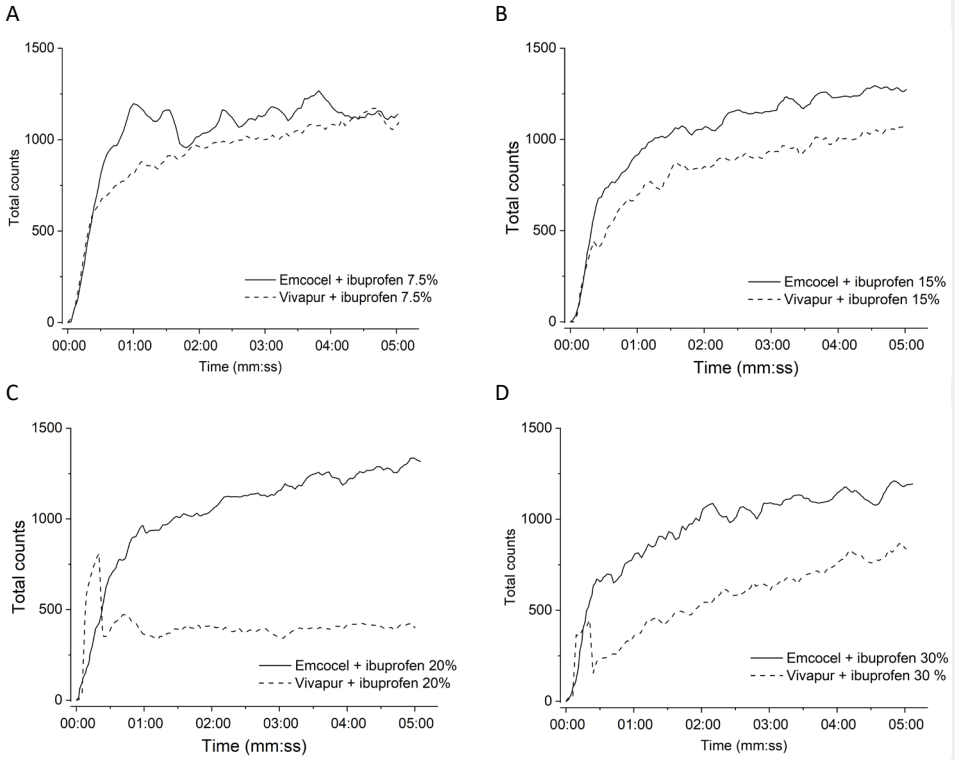

397

398 Figure 3. Focused Beam Reflectance Measurement (FBRM) total counts over time for
399 Vivapur® and Emcocel® tablets containing ibuprofen (A) 7.5 %, (B) 15 %, (C) 20 %, and (D)
400 30% w/w in phosphate buffer pH 7.2 and temperature of 37 °C.

401

402 Due to the variability in the number of counts for each tablet a relative increase in FBRM
403 counts was measured for each tablet to enable comparison between tablets. Figure 8 shows
404 the time necessary to reach 50, 60, 70, 80, 90% total counts. All tablets were tracked for 30
405 minutes. Thus, the total counts of 100% were considered the total counts at 30 min. The
406 overall trend showed a longer time for tablets containing air stream dried MCC compared to
407 spray dried MCC, indicating a slower disintegration rate.

408 **A**

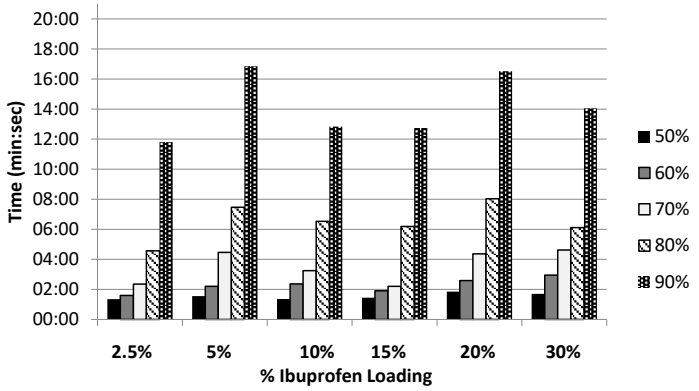

409 **B**

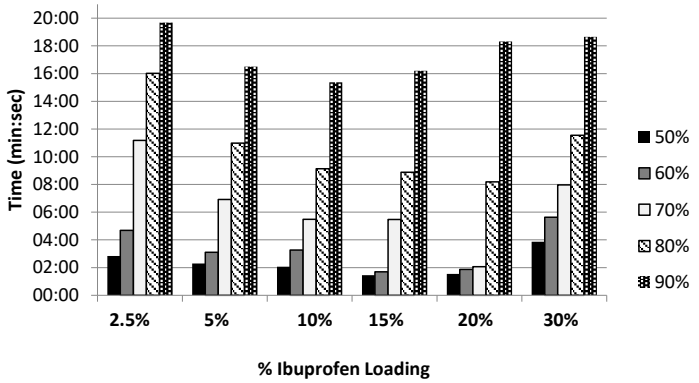

410

411 Figure 8. Time to reach percentage of total particle counts measured by FBRM for tablets
412 after containing (A) spray dried and (B) air stream dried microcrystalline cellulose grades
413 and different ibuprofen w/w/ loadings (2.5 to 30% w/w) disintegrating in phosphate buffer
414 pH 7.2 at 37^{o}C. Percentages expressed relative to total particle counts at 30 mins considered
415 100%.

416

417 An indication of particle size distribution following disintegration was obtained from the
418 FBRM chord length distributions and square weighted chord length distributions (SQWT).
419 Representative tablets with 12.5, 15 % w/w, and 30 % w/w ibuprofen loadings after 5

minutes of dissolution are shown in Figure 9 for the spray dried and air stream dried MCC grades. CLD and SQWCLD for all drug loadings investigated are available in the supplementary material. These distributions are automatically generated for the user by the iC FBRM software. The CLD is comparable to a particle size distribution. This is the number of chord lengths recorded in the measurement scan time in vs the chord length. The SQWCLD is useful for visual comparison of systems by emphasising differences in the course counts (100 – 1000 µm). This is achieved by applying a channel (size intervals or bins) specific weight w_i to counts n_i. The weighted channels y_i are obtained via:

$$y_i = w_i.n_i \quad \text{(Equation 2)}$$

The weights w_i are obtained from the channel midpoints M_i via:

$$w_i = \frac{M_i^{\gamma}}{\sum_{j=1}^{N} M_j^{\gamma}} \cdot N \quad \text{(Equation 3)}$$

Where γ is 2 for the square weight, N is the number of channels, which was 90 in this study, i = 1, 2, …, N and j =1, 2, …, N.

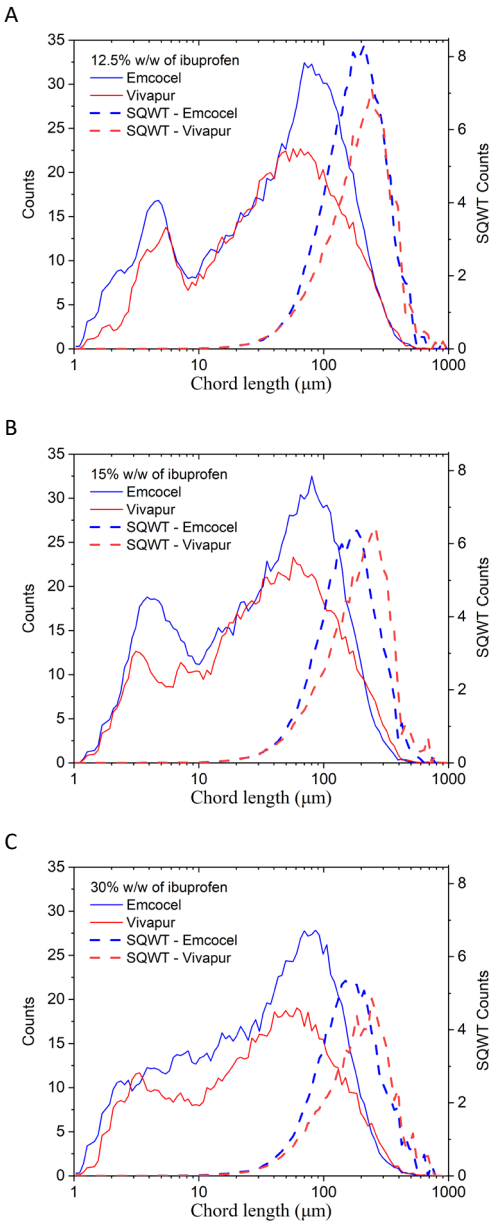

Figure 9. Focused Beam Reflectance Measurement (FBRM) chord length distributions and square weighted chord length distributions for Spray dried MCC® (spray dried MCC) and Air stream dried® (air stream dried MCC) tablets with ibuprofen loading (A) 12.5 %, (B) 15%, and (C) 30 % w/w, 5 minutes after addition to the disintegration medium, phosphate buffer pH 7.2 and temperature of 37 °C.

436 Coarse counts account for a much larger proportion of the mass of material compared with
437 fine counts (1-10 µm). While the CLDs for both systems have a similar shape profile the
438 increased number of total counts and shorter chord length counts was evident for the spray
439 dried compared to the air stream dried MCC. Fine counts may be related to disaggregation
440 of MCC particles which is composed of cellulose fibrils agglomerated into larger particles
441 (Queiroz et al., 2019.) When the square weighted CLDs are compared there is a distinct shift
442 to the right for air stream dried, highlighting the increased particle size present 5 minutes
443 after the tablet addition to the buffer. An increase in fine counts (1-10 µm) present in the
444 spray dried MCC system suggested that tablets of the spray dried MCC disintegrated more
445 effectively than tablets of the air stream dried MCC at a 30 % w/w ibuprofen loading. For
446 loading below the percolation threshold, a similar trend was seen although the shift to the
447 right for air stream dried in the square weighted CLD is less pronounced. This is exemplified
448 by 12.5 % w/w ibuprofen tablets in Figure 9.

449 The plots of chord length distributions at different time points during disintegration for each
450 individual tablet were generated (supplementary data) and selected tablets shown in Figure
451 10. The increase in counts over time happens similarly across all chord lengths for a same
452 tablet, i.e. the distribution did not show a shape change at different time points.
453 Interestingly, the increase in count is clearly more significant up to 5 min. After that, the
454 change is counts is comparatively very small.

455

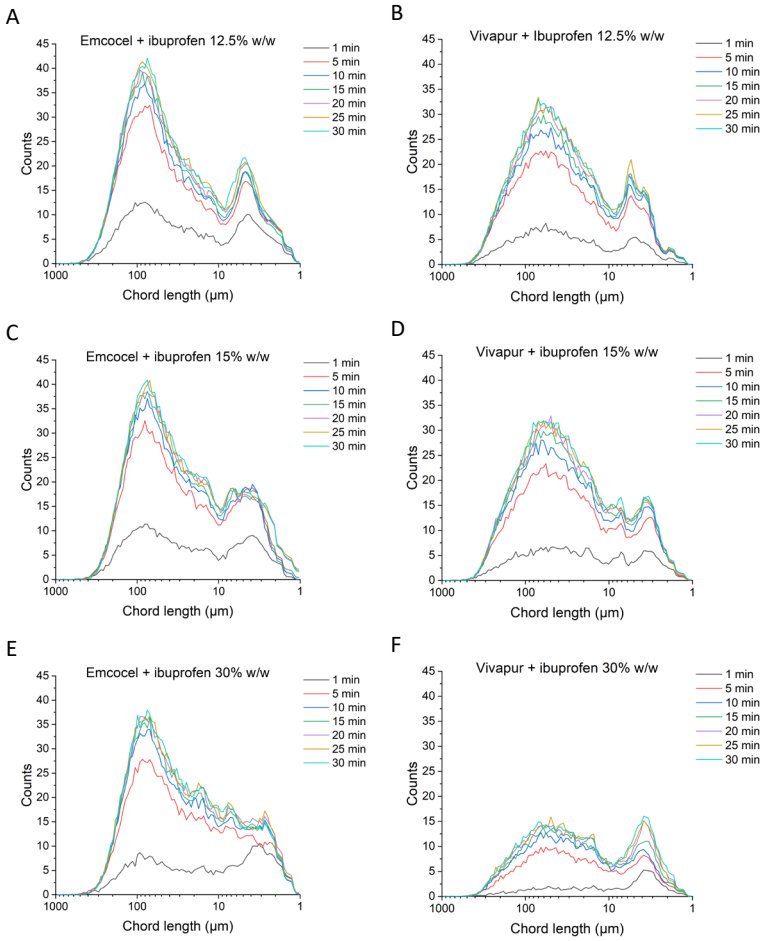

456 Figure 10. Focused Beam Reflectance Measurement (FBRM) chord length distributions for
457 tablets with ibuprofen loadings of 12.5 %, 15%, and 30 % w/w and (A, C, and D) Spray dried
458 MCC® (spray dried MCC) and (B, D, and F) Air stream dried® (air stream dried MCC),
459 respectively, at different times after addition to the disintegration medium, phosphate
460 buffer pH 7.2 and temperature of 37 °C. This analysis is available for tablets at all drug
461 loadings in the supplementary material.

462

463 Based on the results shown in Figure 11, the cumulative drug release at 5 min was plotted
464 against IBU concentration in order to investigate the differences in drug release below and
465 above the threshold following tablet disintegration (Figure 5). Interestingly, after 5 min time

point the pharmacopeial disintegration tested showed complete disintegration. Similar graphical approaches have been previously used to determine the percolation threshold from disintegration and dissolution (Kimura et al., 2007a; Wenzel et al., 2017).

Cumulative release decreased sharply from 2.5 to 15% w/w of ibuprofen loading. However, at drug loadings above the percolation threshold (20% w/w and 30% w/w IBU) the reduction in drug release with increase in drug loading was decreased. Tablets containing the air stream dried MCC showed significantly lower drug release for all drug loadings in comparison to tablets containing the spray dried MCC. These findings showed the change in dissolution behaviour at drug concentrations above and below the predicted percolation threshold following tablet disintegration.

477

A

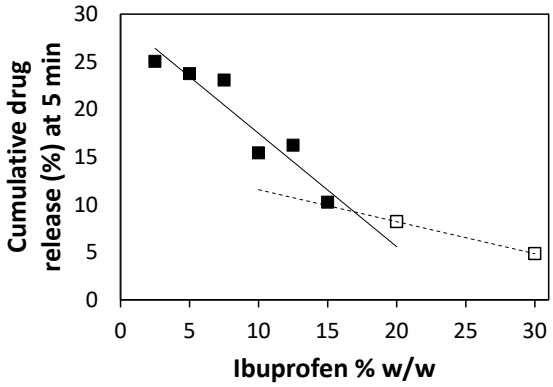

B

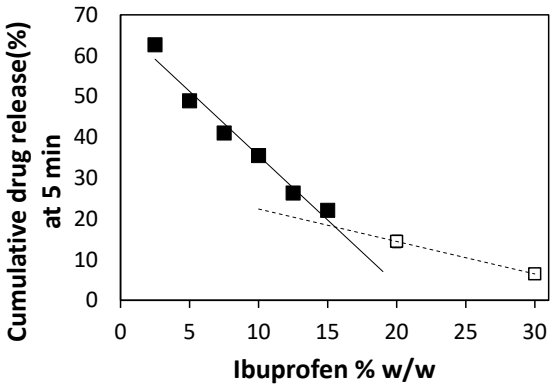

478

479 Figure 11. Estimation of percolation threshold based on the dissolution cumulative release
480 of ibuprofen from the tablets containing (A) air stream dried and (B) spray dried
481 microcrystalline cellulose, at 5 min of dissolution. The time of 5 minutes was chosen as all
482 tablets had disintegrated at 5 min based on FBRM results.

483

484 .

485

486 4.5 PVM analysis

487 PVM analysis was performed to provide real-time images of particles in dissolution medium
488 during tablet disintegration. Besides the images, PVM relative backscatter index was used as
489 a quantitative measure of disintegration. Initially, images were collected using the PVM
490 probe for ibuprofen powder and both MCC only tablets in buffer. The ibuprofen particles
491 had a distinct rod-shaped habit (Figure 12a). Dispersed ibuprofen powder was present as
492 both discrete particles and aggregates. The ibuprofen particles appeared to be between 100
493 and 300 µm in length and 30 and 50 µm in width. When compared with the particle size for
494 the dry powder from laser diffraction (Table 1), where the D50 was 55 µm, it appears that
495 larger ibuprofen particles in the PVM images may be aggregates.
496 PVM images of the disintegrated spray dried MCC tablet (Figure 12b) indicated that fine
497 material was present along with uniform distinct particles having a rough surface. Images of
498 disintegrated air stream dried MCC tablet (Figure 12c) are similar to spray dried MCC. These
499 images would support the presence of fine particles observed during FBRM analysis, Figures
500 9 and 10. These appeared to be rod shaped particles present which are similar in
501 appearance to the ibuprofen particles.
502

503

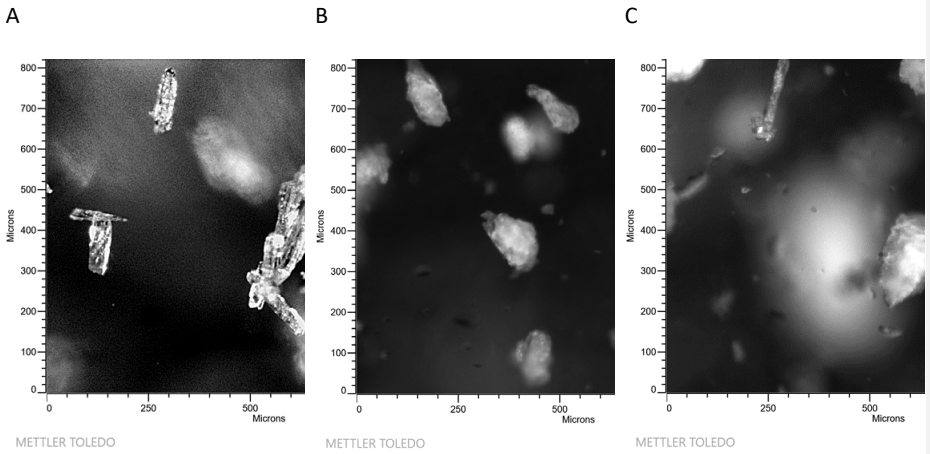

504 Figure 12. PVM images of (A) ibuprofen powder, and (B) Spray dried MCC® and (C) Air
505 stream dried® particles following tablet disintegration in phosphate buffer pH7.2 and
506 temperature of 37 °C.

507

508 Side by side comparison of PVM images of disintegrated tablets containing spray dried and
509 air stream dried MCC with equivalent ibuprofen loading showed that it is difficult to
510 distinguish definite differences between the two systems. One difference noted was that air
511 stream dried tablets showed more elongated particles (Figure 13). There are rod shaped
512 particles present in the air stream dried suspension (Figure 12), hence it was not possible to
513 distinguish whether this rod-shaped material following the 15% w/w ibuprofen tablet
514 disintegration is ibuprofen or MCC.

A B

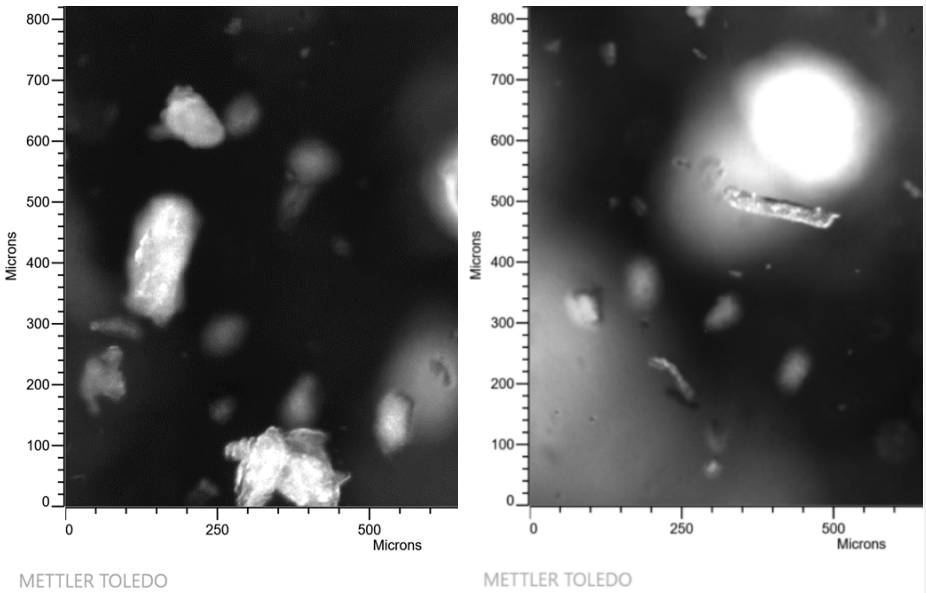

Figure 13. Representative PVM images of particles following disintegration of (A) spray dried MCC and (B) air stream dried MCC tablets with a 15 % w/w ibuprofen loading in phosphate buffer pH7.2 and temperature of 37 °C.

Relative Backscatter Index (RBI) measured by PVM is the relationship between the incident and the detected light. As disintegration progresses the number of particles in the media increases due to fragmentation of larger particles to smaller particles and RBI increases. The change in the PVM RBI versus time during disintegration does indicate differences for tablets containing 20% and 30% ibuprofen loading tablets compared to tablets containing lower ibuprofen loadings (Figure 14). For ibuprofen loadings below the percolation threshold the RBI for both spray dried and air stream dried MCC tablets was similar. RBI increased to a greater extent for the spray dried MCC tablets with increased drug loadings compared to air stream dried MCC (Figure 14d). The air stream dried MCC tablets with a 20 and 30% w/w ibuprofen has a significantly lower final RBI during disintegration.

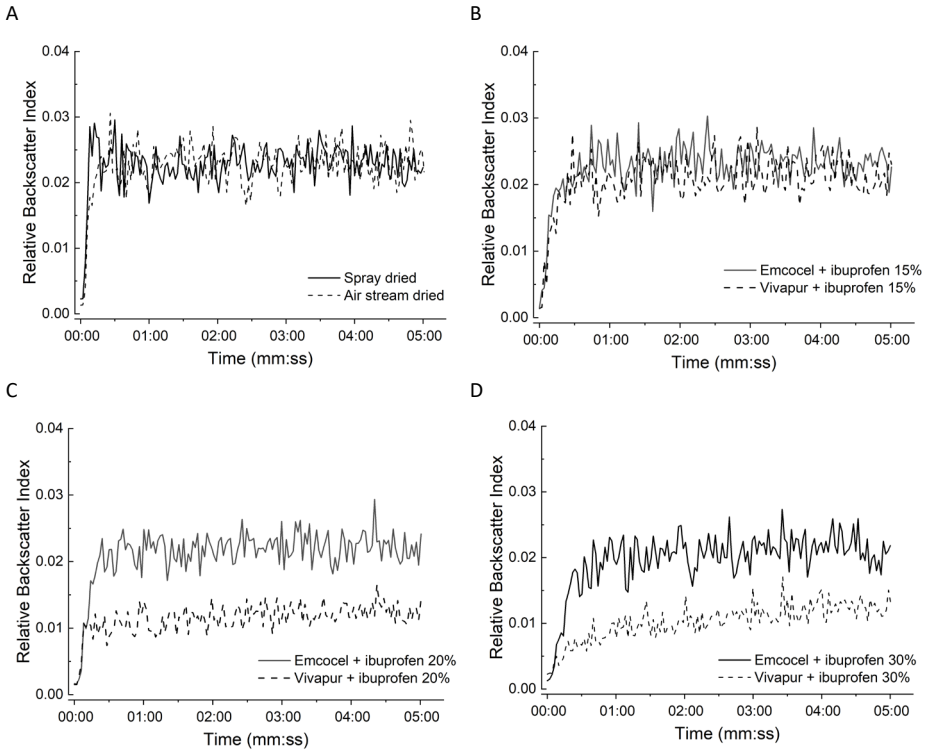

Figure 14. Relative Backscatter Index (RBI) vs time following disintegration of Spray dried MCC® and Air stream dried® tablets (A) 0% w/w, (B) 15% w/w, (C) 20% w/w and (D) 30% w/w ibuprofen in phosphate buffer pH7.2 and temperature of 37 °C.

5. DISCUSSION

The research presented was conducted to better understand whether a percolation threshold determined from compaction data can translate to experimental tablet disintegration and dissolution data and the effect of the presence of a critical drug load (percolation threshold) on tablet disintegration and drug dissolution.

Previous studies determined a percolation threshold value from disintegration and dissolution experimental data (Kimura et al., 2007a; Stillhart et al., 2017; Wenzel et al., 2017). The earlier study was focused on predicting mathematically and confirming

542 experimentally the existence of a percolation threshold from a blend properties and
543 compaction behaviour perspective. In the present study, disintegration and dissolution
544 experiments were carried out to experimentally to confirm the percolation threshold, which
545 had been predicted using an statistical hybrid model (Queiroz et al., 2019).
546 Dissolution testing confirmed the presence of the percolation threshold in the region
547 previously reported. The change in behaviour above the percolation threshold was observed
548 during dissolution; % drug released at 5 min following tablet disintegration (Figure 11) and
549 time to achieve complete dissolution (Figure 4). Blends above the percolation threshold
550 showed slower dissolution profiles. Kimura, Betz and Leuenberger, 2007 also revealed a
551 decreased disintegration performance above the critical loading of a poorly water-soluble
552 drug. In the case of tablets containing MCC and ibuprofen, it was hypothesised that the
553 connected MCC particles would form the water-conducting clusters promoting
554 disintegration. Above the threshold predicted a continuous cluster of ibuprofen particles is
555 formed. Relative to MCC, ibuprofen is poorly water soluble, and the formation of
556 continuous ibuprofen clusters would decrease disintegration. Thus, the explanation for the
557 reduction in dissolution above the percolation threshold can be attributed to the combined
558 effect of decreased drug surface area to mass due to the presence of continuous clusters
559 evidenced by Raman imaging and a change in the disintegration process.
560 In this study, Raman imaging and image domain analysis were combined to confirm
561 percolation threshold in pharmaceutical tablets. The methodology developed confirmed the
562 percolation threshold previously predicted for the binary blend investigated (Queiroz et al.,
563 2019) by an increasing number of drug cluster up to the percolation threshold and reduction
564 above due to the formation of continuous clusters. For the drug loading above 15%, the
565 number of ibuprofen domains dramatically decreased, and their equivalent circle diameter

566 increased which confirms the cluster formation and would contribute to a slower rate of
567 ibuprofen dissolution due to a reduced surface area to mass ratio.
568 The influence of the presence of continuous ibuprofen clusters on tablet disintegration was
569 difficult to establish by pharmacopoeial disintegration testing. However, the use of FBRM
570 and PVM to determine the tablet disintegration behaviour with respect to drug loading
571 demonstrated a change in behaviour above the percolation threshold, particularly for
572 tablets containing air stream dried MCC (Figures 7 and 14). PVM images of disintegration
573 showed an omnidirectional enlargement of particles prior fragmentation of the tablet. This
574 is a typical behaviour of immediate-release tablets and characterizes the swelling
575 disintegration mechanism (Caramella et al., 1988). The dissolution of the disintegrated
576 particles could not be observed by FBRM nor PVM due to similarity in morphology of the
577 disaggregated MCC particles and ibuprofen particles (Figure 13) and the insoluble nature of
578 MCC in the disintegration medium. However, it may be possible to monitor drug dissolution
579 for formulations with high drug loadings and soluble excipients, such as lactose, using PVM
580 and FBRM techniques.
581 The secondary objective of this study was to investigate the influence of MCC grade on
582 disintegration and dissolution behaviour relative to the percolation threshold. Despite the
583 MCC grades having similar bulk properties, the interaction of each grade with the model
584 drug ibuprofen resulted in differing dissolution behaviour. In all cases, the tablets containing
585 the air stream dried grade showed slower disintegration and dissolution rates. Air stream
586 dried MCC tablets showed a reduction in disintegration rate above the percolation threshold
587 value while spray dried MCC did not (Figure 6 and 14). These tablets resulted in the slower
588 dissolution rates (Figure 4) across all drug loading. Tablets produced from the air stream
589 dried MCC grade were slightly less porous (Table 2). Tablet porosity is a function of drug

590 loading and for poorly compressible drugs reduced above the percolation threshold value,
591 but also a dependent on the grade of MCC employed (Queiroz et al., 2019). Differences in
592 MCC crystallinity has also been related to lower swelling of MCC; polymers with less dense
593 crystalline regions were observed to swell more as they are more accessible for the water
594 molecules and the cohesive forces between the chain segments are weaker in comparison
595 to the crystalline domains (Desai et al., 2016; Schott, 1992). Further studies are required to
596 determine the exact mechanisms causing in the reduced dissolution rates for tablets
597 containing air stream dried MCC compared to the spray dried grade.
598 It was challenging to discriminate between the effects of tablet porosity and percolation
599 threshold in relation to tablet disintegration. The compaction parameters and bonding
600 mechanism of particles during compaction directly impact tablet porosity, the ingress of the
601 disintegration medium, MCC swelling and hence tablet disintegration (Yassin et al., 2015).
602 Despite confounding differences observed in tablet porosity in this study, a clear step
603 change in dissolution behaviour was observed for tablets with drug loadings above the
604 percolation threshold.
605

606 **6. CONCLUSIONS**

607 Dissolution data showed that a percolation threshold value previously determined for
608 ibuprofen/MCC binary blends, from compaction data, translated to tablet dissolution data.
609 Slower ibuprofen dissolution behaviour was observed for tablets above the predetermined
610 percolation threshold level and confirmed the presence of the percolation threshold
611 relevant to dissolution. In addition, slower dissolution was observed for all tablets
612 containing an air stream dried MCC grade compared to a spray dried MCC grade. FBRM and

PVM showed less efficient disintegration above the percolation threshold for tablets containing air stream dried MCC. The results experimentally demonstrate that both larger drug domains, quantified by Raman imaging, and a less efficient tablet disintegration (in the case of air stream dried MCC) measured by FBRM and PVM contributed to slower ibuprofen dissolution profiles above the percolation threshold.

Acknowledgements

Funding: This publication has emanated from research supported in part by a research grant from Science Foundation Ireland (SFI) and is co-funded under the European Regional Development Fund [grant number 12/RC/2275].

Dissolution tests were carried out by Ms. Roisin Keane and Ailbhe Kearney, School of Pharmacy University College Cork.

625 **REFERENCES**

626 Agarwal, U.P., Reiner, R.S., Ralph, S.A., 2010. Cellulose I crystallinity determination using FT-
627 Raman spectroscopy: Univariate and multivariate methods. Cellulose 17, 721–733.
628 https://doi.org/10.1007/s10570-010-9420-z

629 Al-Karawi, C., Cech, T., Bang, F., Leopold, C.S., 2018. Investigation of the tableting behavior
630 of Ibuprofen DC 85 W. Drug Dev. Ind. Pharm. 44, 1262–1272.
631 https://doi.org/10.1080/03639045.2018.1442846

632 Al-khattawi, A., Alyami, H., Townsend, B., Ma, X., Mohammed, A.R., 2014. Evidence-based
633 nanoscopic and molecular framework for excipient functionality in compressed orally
634 disintegrating tablets. PLoS One 9, e101369.
635 https://doi.org/10.1371/journal.pone.0101369

636 Ali, S.M., Bonnier, F., Lambkin, H., Flynn, K., McDonagh, V., Healy, C., Lee, T.C., Lyng, F.M.,
637 Byrne, H.J., 2013. A comparison of Raman, FTIR and ATR-FTIR micro spectroscopy for
638 imaging human skin tissue sections. Anal. Methods 5, 2281–2291.
639 https://doi.org/10.1039/c3ay40185e

640 Barrett, M., Hao, H., Maher, A., Hodnett, K., Glennon, B., Croker, D., 2011. In Situ Monitoring
641 of Supersaturation and Polymorphic Form of Piracetam during Batch Cooling
642 Crystallization. Org. Process Res. Dev. 15, 681–687.
643 https://doi.org/10.1021/op2000628

644 Barrett, P., Glennon, B., 2002. Characterizing the Metastable Zone Width and Solubility
645 Curve Using Lasentec FBRM and PVM. Chem. Eng. Res. Des. 80, 799–805.
646 https://doi.org/https://doi.org/10.1205/026387602320776876

647 Barrett, P., Glennon, B., 1999. In-line FBRM Monitoring of Particle Size in Dilute Agitated
648 Suspensions. Part. Part. Syst. Charact. 16, 207–211. https://doi.org/10.1002/(SICI)1521-
649 4117(199910)16:5<207::AID-PPSC207>3.0.CO;2-U

650 Bonny, J.D., Leuenberger, H., 1993. Matrix type controlled release systems II. Percolation
651 effects in non-swellable matrices. Pharm. Acta Helv. 68, 25–33.
652 https://doi.org/10.1016/0031-6865(93)90005-Q

653 Bonny, J.D., Leuenberger, H., 1991. Matrix type controlled release systems: I. Effect of
654 percolation on drug dissolution kinetics. Pharm. Acta Helv. 66, 160–164.

655 Caramella, C., Colombo, P., Conte, U., Ferrari, F., Gazzaniga, A., LaManna, A., Peppas, N.A.,
656 1988. A physical analysis of the phenomenon of tablet disintegration. Int. J. Pharm. 44,
657 177–186. https://doi.org/10.1016/0378-5173(88)90114-7

658 Castellan, A., Ruggiero, R., Frollini, E., Ramos, L.A., Chirat, C., 2007. Studies on fluorescence
659 of cellulosics. Holzforschung 61, 504–508. https://doi.org/10.1515/HF.2007.090

660 Chan, K.L.A., Elkhider, N., Kazarian, S.G., 2005. Spectroscopic imaging of compacted
661 pharmaceutical tablets. Chem. Eng. Res. Des. 83, 1303–1310.
662 https://doi.org/10.1205/cherd.05088

663 Council of Europe, 2019. European Pharmacopoeia (Ph. Eur.).

664 Coutant, C., Skibic, M., Doddridge, G., Kemp, C., Sperry, D., 2010. In Vitro Monitoring of
665 Dissolution of an Immediate Release Tablet by Focused Beam Reflectance
666 Measurement. Mol. Pharm. 7. https://doi.org/10.1021/mp1001476

667 Dabbagh, M.A., Taghipour, B., 2007. Investigation of Solid Dispersion Technique in
668 Improvement of Physicochemical Characteristics of Ibuprofen Powder. Iran. J. Pharm.
669 Sci. 3, 69–76.

670 Desai, P.M., Liew, C.V., Heng, P.W.S., 2016. Review of Disintegrants and the Disintegration
671 Phenomena. J. Pharm. Sci. 105, 2545–2555.
672 https://doi.org/10.1016/j.xphs.2015.12.019

673 Dressman, J., Krämer, J., 2005. Pharmaceutical dissolution testing, Pharmaceutical
674 Dissolution Testing. Taylor & Francis. https://doi.org/10.1016/0168-3659(94)90064-7

675 Gregory, J., 2009. Monitoring particle aggregation processes. Adv. Colloid Interface Sci. 147–
676 148, 109–123. https://doi.org/10.1016/j.cis.2008.09.003

677 Han, J.-H., Ferro, L., Vaidya, A., George, S., Pandey, A., Smith, B., 2009. Real-time Study of
678 Disintegration and Dissolution in Solid Oral Dosage Forms with Focused Beam
679 Reflectance Measurement (FBRM) Technology, in: AAPS Annual Meeting and
680 Exposition Los Angeles, CA.

681 Hartwig, A., Hass, R., 2018. Monitoring Lactose Crystallization at Industrially Relevant
682 Concentrations by Photon Density Wave Spectroscopy. Chem. Eng. Technol. 41, 1139–
683 1146. https://doi.org/10.1002/ceat.201700685

684 Huang, J., Goolcharran, C., Ghosh, K., 2011. A Quality by Design approach to investigate
685 tablet dissolution shift upon accelerated stability by multivariate methods. Eur. J.
686 Pharm. Biopharm. 78, 141–150. https://doi.org/10.1016/j.ejpb.2010.12.012

687 Ibrahim, H.G., 1985. Observations on the dissolution behavior of a tablet formulation: Effect
688 of compression forces. J. Pharm. Sci. 74, 575–577.
689 https://doi.org/10.1002/jps.2600740519

690 International Council for Harmonisation, 2012. ICH Q 11 Development and manufacture of
691 drug substances (chemical entities and biotechnological/biological entities).

692 International Council for Harmonisation, 2008. ICH Q10 Pharmaceutical quality system.

693 International Council for Harmonisation, 2005a. ICH Q8 (R2) Pharmaceutical development.

694 International Council for Harmonisation, 2005b. ICH Q9 Quality risk management.

695 Jiang, M., Zhu, X., Molaro, M.C., Rasche, M.L., Zhang, H., Chadwick, K., Raimondo, D.M., Kim,
696 K.-K.K., Zhou, L., Zhu, Z., Wong, M.H., O'Grady, D., Hebrault, D., Tedesco, J., Braatz,
697 R.D., 2014. Modification of Crystal Shape through Deep Temperature Cycling. Ind. Eng.
698 Chem. Res. 53, 5325–5336. https://doi.org/10.1021/ie400859d

699 Kawabata, Y., Wada, K., Nakatani, M., Yamada, S., Onoue, S., 2011. Formulation design for
700 poorly water-soluble drugs based on biopharmaceutics classification system: Basic
701 approaches and practical applications. Int. J. Pharm.
702 https://doi.org/10.1016/j.ijpharm.2011.08.032

703 Kazarian, S.G., Ewing, A. V., 2013. Applications of Fourier transform infrared spectroscopic
704 imaging to tablet dissolution and drug release. Expert Opin. Drug Deliv.
705 https://doi.org/10.1517/17425247.2013.801452

706 Kimura, G., Betz, G., Leuenberger, H., 2007a. Influence of loading volume of mefenamic acid
707 on granules and tablet characteristics using a compaction simulator. Pharm. Dev.
708 Technol. 12, 627–635. https://doi.org/10.1080/10837450701634037

709 Kimura, G., Betz, G., Leuenberger, H., 2007b. Influence of Loading Volume of Mefenamic
710 Acid on Granules and Tablet Characteristics Using a Compaction Simulator. Pharm. Dev.
711 Technol. 12, 627–635. https://doi.org/10.1080/10837450701634037

712 Kimura, G., Puchkov, M., Leuenberger, H., 2013. An attempt to calculate in silico
713 disintegration time of tablets containing mefenamic acid, a low water-soluble drug. J.
714 Pharm. Sci. 102, 2166–2178. https://doi.org/10.1002/jps.23541

715 Leuenberger, H., 1999. Application of percolation theory in powder technology. Adv.
716 Powder Technol. https://doi.org/10.1163/156855299X00190

717 Liu, L.X., Marziano, I., Bentham, A.C., Litster, J.D., E.T.White, Howes, T., 2008. Effect of
718 particle properties on the flowability of ibuprofen powders. Int. J. Pharm. 362, 109–
719 117. https://doi.org/10.1016/j.ijpharm.2008.06.023

720 Liu, X., Sun, D., Wang, F., Wu, Y., Chen, Y., Wang, L., 2011. Monitoring of antisolvent
721 crystallization of sodium scutellarein by combined FBRM–PVM–NIR. J. Pharm. Sci. 100,
722 2452–2459. https://doi.org/10.1002/jps.22439

723 Lowenthal, W., 1973. Mechanism of action of tablet disintegrants. Pharm. Acta Helv.

724 Markl, D., Zeitler, J.A., 2017. A Review of Disintegration Mechanisms and Measurement
725 Techniques. Pharm. Res. 34, 890–917. https://doi.org/10.1007/s11095-017-2129-z

726 Menning, M., 2016. Towards a Fundamental Understanding of Particle Kinetics through
727 Dynamic Characterization of Pharmaceutical Solid Dosage Forms. University College
728 Dublin.

729 Metzler, C., Bullard, J.W., Waldo, M., McCarty, K., Do, M., 2017. Using a Focused Beam
730 Reflectance Measurement (FBRM) Probe to Characterize Tablet Disintegration Behavior
731 As a Function of Drug Product Processing Conditions, in: AIChE Annual Meeting,
732 Minneapolis. p. 720(a).

733 Miller, T.C., Havrilla, G.J., 2005. Elemental imaging for pharmaceutical tablet formulation
734 analysis by micro X-ray fluorescence. Powder Diffr. 20, 153–157.
735 https://doi.org/10.1154/1.1913720

736 Mitchell, N.A., Frawley, P.J., Ó'Ciardhá, C.T., 2011. Nucleation kinetics of paracetamol–
737 ethanol solutions from induction time experiments using Lasentec FBRM®. J. Cryst.
738 Growth 321, 91–99. https://doi.org/https://doi.org/10.1016/j.jcrysgro.2011.02.027

739 Nickerson, B., Kong, A., Gerst, P., Kao, S., 2018. Correlation of dissolution and disintegration
740 results for an immediate-release tablet. J. Pharm. Biomed. Anal. 150, 333–340.
741 https://doi.org/10.1016/j.jpba.2017.12.017

742 Queiroz, A.L.P., Faisal, W., Devine, K., Garvie-Cook, H., Vucen, S., Crean, A.M., 2019. The
743 application of percolation threshold theory to predict compaction behaviour of
744 pharmaceutical powder blends. Powder Technol. 354, 188–198.
745 https://doi.org/10.1016/j.powtec.2019.05.027

746 Rowe, R.C., Sheskey, P.J., Quinn, M.E. (Eds.), 2009. Handbook of pharmaceutical excipients,
747 6th editio. ed. Pharmaceutical Press.

748 Schott, H., 1992. Swelling kinetics of polymers. J. Macromol. Sci. Part B 31, 1–9.
749 https://doi.org/10.1080/00222349208215453

750 Simon, M., Wood, B., Ferguson, S., Glennon, B., Jones, R.C., 2019. Diastereomeric salt
751 crystallization of chiral molecules via sequential coupled-Batch operation. AIChE J. 65,
752 604–616. https://doi.org/10.1002/aic.16466

753 Simone, E., Sal, A., Nagy, Z., 2015. In Situ Monitoring of Polymorphic Transformations Using
754 a Composite Sensor Array of Raman, NIR, and ATR-UV/vis Spectroscopy, FBRM, and
755 PVM for an Intelligent Decision Support System. Org. Process Res. Dev. 19, 167–177.
756 https://doi.org/10.1021/op5000122

757 Stillhart, C., Parrott, N.J., Lindenberg, M., Chalus, P., Bentley, D., Szepes, A., 2017.
758 Characterising Drug Release from Immediate-Release Formulations of a Poorly Soluble
759 Compound, Basmisanil, Through Absorption Modelling and Dissolution Testing. AAPS J.
760 19, 827–836. https://doi.org/10.1208/s12248-017-0060-1

761 Sütő, B., Berkó, S., Kozma, G., Kukovecz, Á., Budai-Szucs, M., Erös, G., Kemény, L., Sztojkov-
762 Ivanov, A., Gáspár, R., Csányi, E., 2016. Development of ibuprofen-loaded
763 nanostructured lipid carrier-based gels: Characterization and investigation of in vitro
764 and in vivo penetration through the skin. Int. J. Nanomedicine 11, 1201–1212.
765 https://doi.org/10.2147/IJN.S99198

766 Wenzel, T., Stillhart, C., Kleinebudde, P., Szepes, A., 2017. Influence of drug load on
767 dissolution behavior of tablets containing a poorly water-soluble drug: estimation of
768 the percolation threshold. Drug Dev. Ind. Pharm. 43, 1265–1275.
769 https://doi.org/10.1080/03639045.2017.1313856

770 Werner, P., Münzberg, M., Hass, R., Reich, O., 2017. Process analytical approaches for the
771 coil-to-globule transition of poly(N-isopropylacrylamide) in a concentrated aqueous
772 suspension. Anal. Bioanal. Chem. 409, 807–819. https://doi.org/10.1007/s00216-016-
773 0050-7

774 Wiley, J.H., Atalla, R.H., 1987. Band assignments in the raman spectra of celluloses.
775 Carbohydr. Res. 160, 113–129. https://doi.org/10.1016/0008-6215(87)80306-3

776 Yassin, S., Goodwin, D.J., Anderson, A., Sibik, J., Wilson, D.I., Gladden, L.F., Zeitler, J.A., 2015.
777 The Disintegration Process in Microcrystalline Cellulose Based Tablets, Part 1: Influence
778 of Temperature, Porosity and Superdisintegrants. J. Pharm. Sci. 104, 3440–3450.
779 https://doi.org/10.1002/jps.24544

780 Zhang, L., Henson, M.J., Sekulic, S.S., 2005. Multivariate data analysis for Raman imaging of a
781 model pharmaceutical tablet. Anal. Chim. Acta 545, 262–278.
782 https://doi.org/10.1016/j.aca.2005.04.080

783 Zhong, L., Gao, L., Li, L., Zang, H., 2020. Trends-process analytical technology in solid oral
784 dosage manufacturing. Eur. J. Pharm. Biopharm. 153, 187–199.
785 https://doi.org/10.1016/j.ejpb.2020.06.008

786

787

SUPPLEMENTARY MATERIAL

A

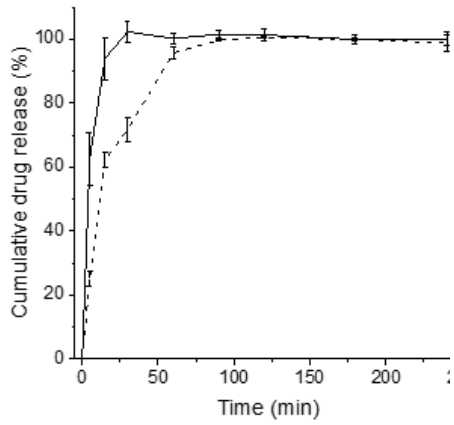

B

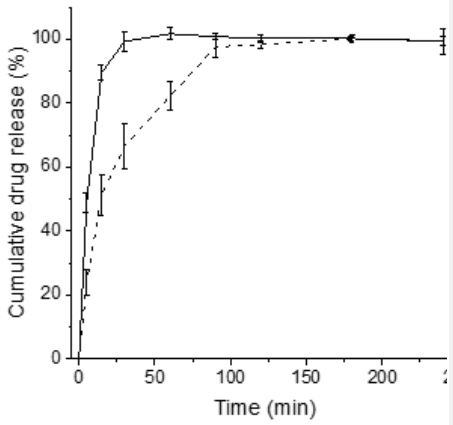

C

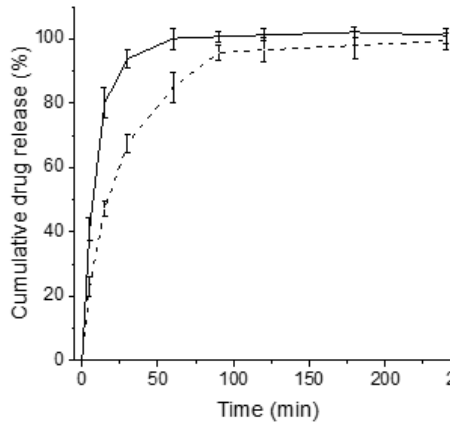

D

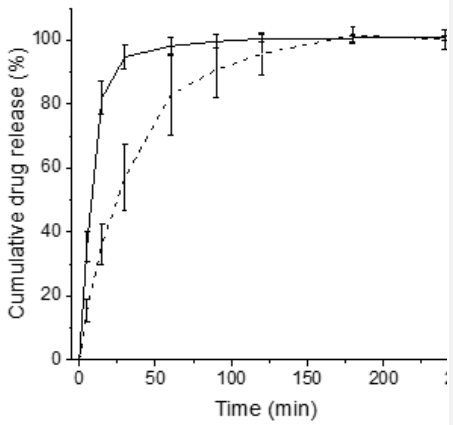

E

F

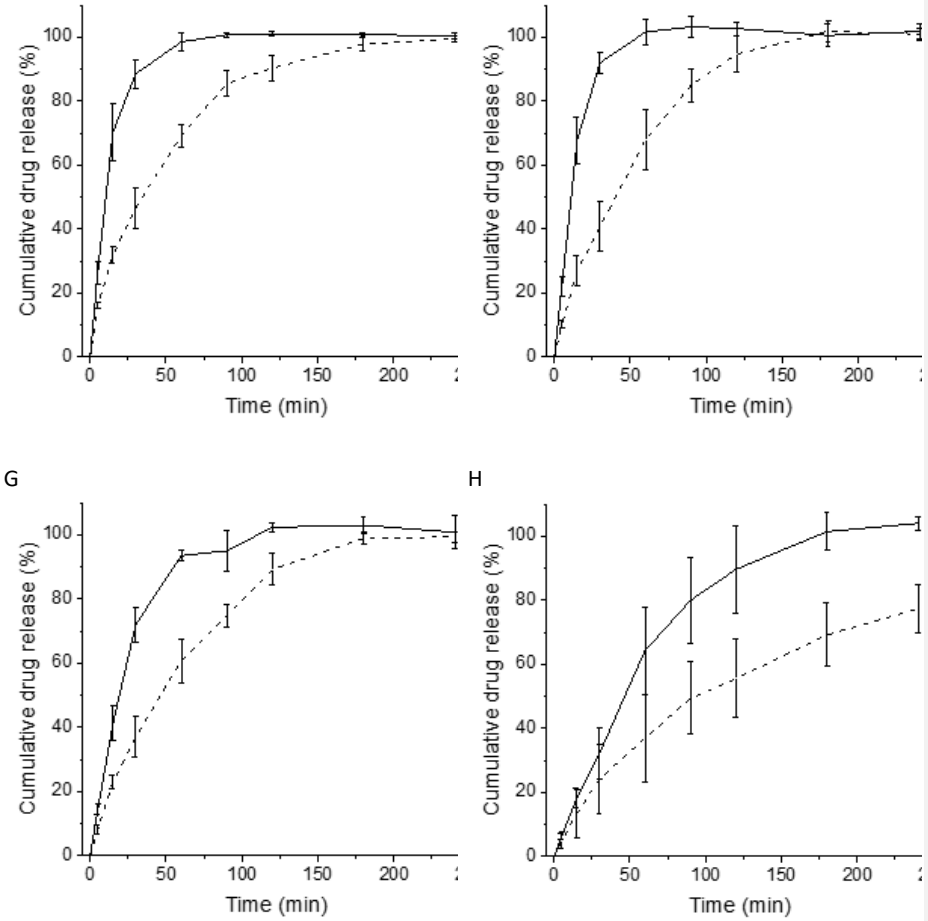

789 Figure SM-1. Dissolution profiles of tablets containing spray dried MCC (Emcocel®) (solid
790 line) and air stream dried MCC (Vivapur®) (dashed line) containing ibuprofen (a) 2.5 %, (b) 5
791 %, (c) 7.5 %, (d) 10 %, (e) 12.5 %, (f) 15 %, (g) 20 %, and (h) 30 % w/w. Dashed and solid lines
792 correspond to air stream and spray dried MCCs, respectively. Dissolution was performed in
793 phosphate buffer pH 7.2 at 37°C. Average values shown with y-error bars indicating
794 standard deviation, n= 5.

795

Ibuprofen loading (%w/w)	Air stream dried	Spray dried
2.5	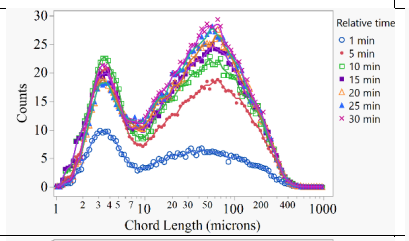	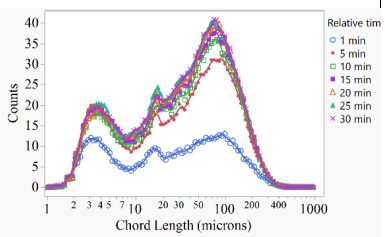
5	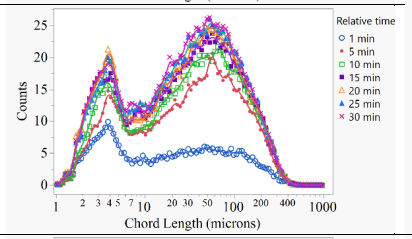	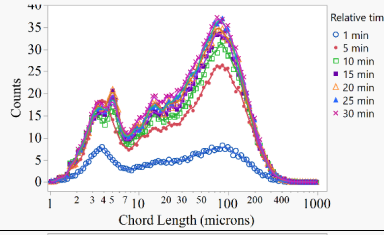
7.5	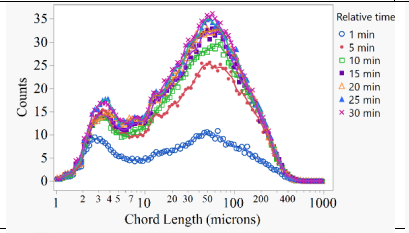	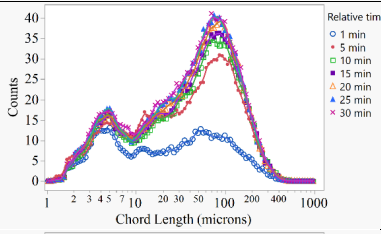
10	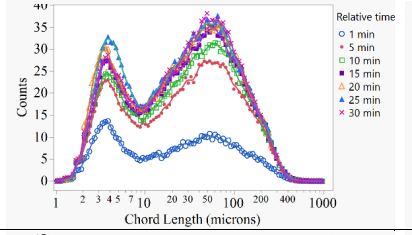	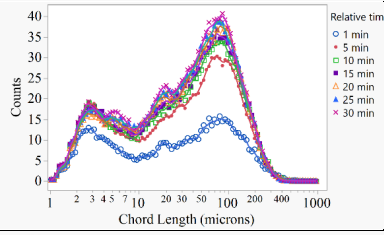
12.5	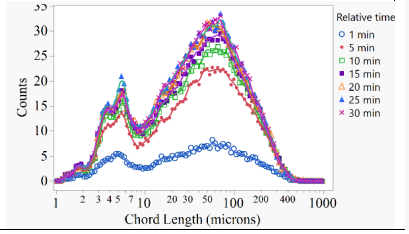	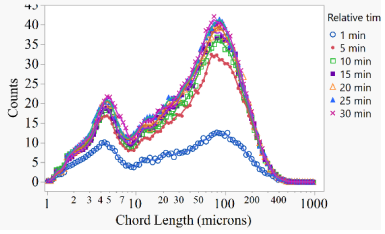

15	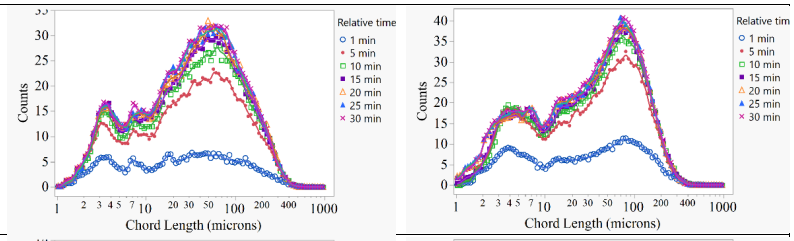
20	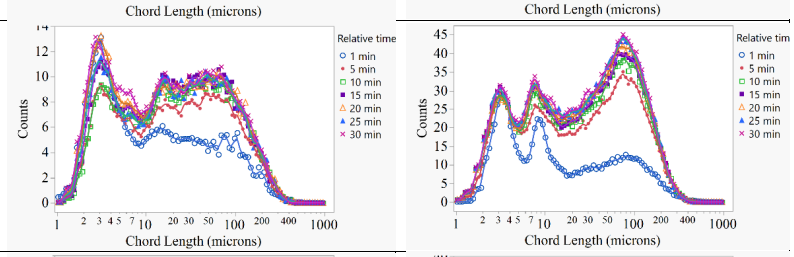
30	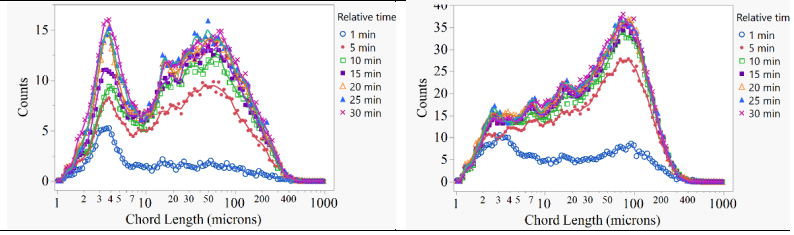

Figure SM-2. Focused Beam Reflectance Measurement (FBRM) chord length distributions for tablets with ibuprofen loadings of 2.5 % - 30 % w/w spray dried MCC (Emcocel®) and air stream dried MCC (Vivapur®), respectively, at different time ponts after addition to the disintegration medium, phosphate buffer pH 7.2 and temperature of 37 °C.

A

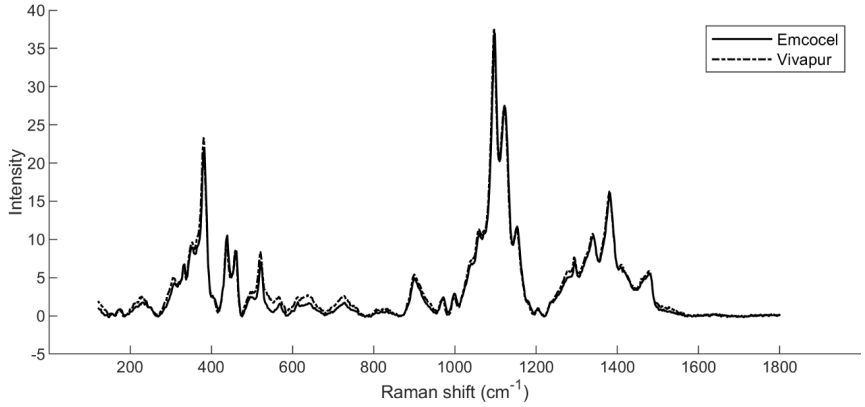
Emcocel
Vivapur
Intensity
Raman shift (cm-1)

B

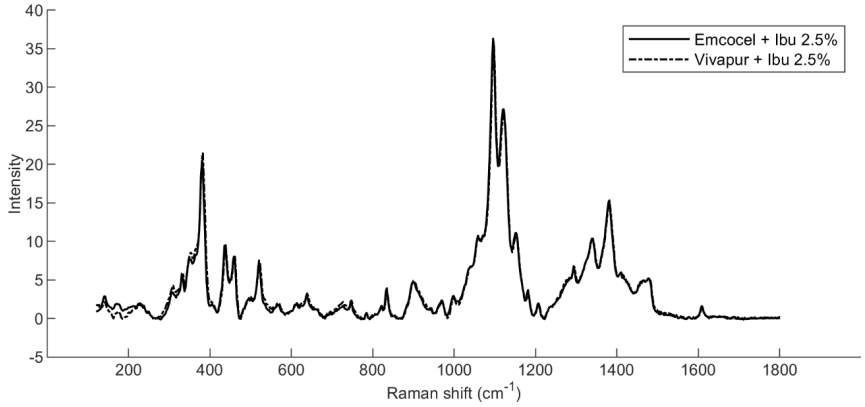
Emcocel + Ibu 2.5%
Vivapur + Ibu 2.5%
Intensity
Raman shift (cm-1)

801

C

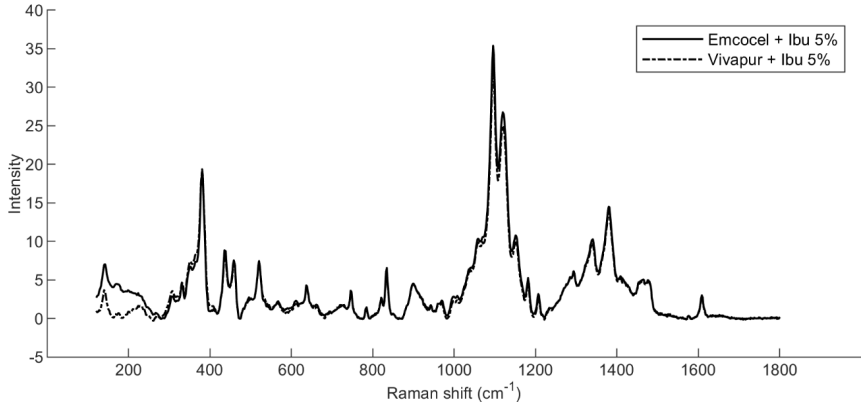
Emcocel + Ibu 5%
Vivapur + Ibu 5%
Intensity
Raman shift (cm-1)

D

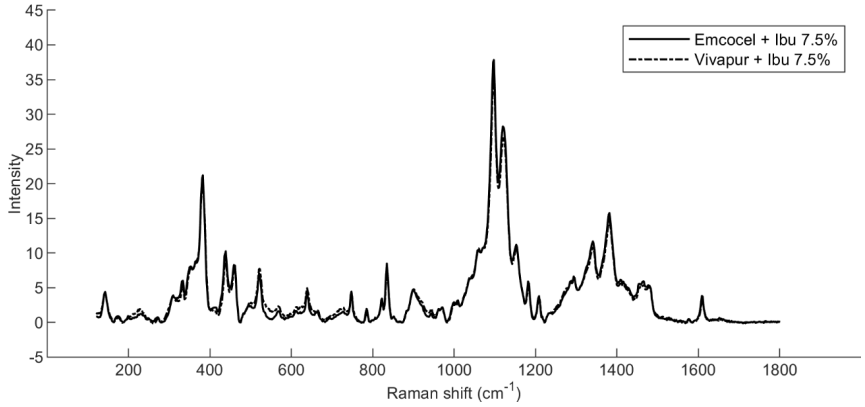
Emcocel + Ibu 7.5%
Vivapur + Ibu 7.5%
Intensity
Raman shift (cm-1)

802

E

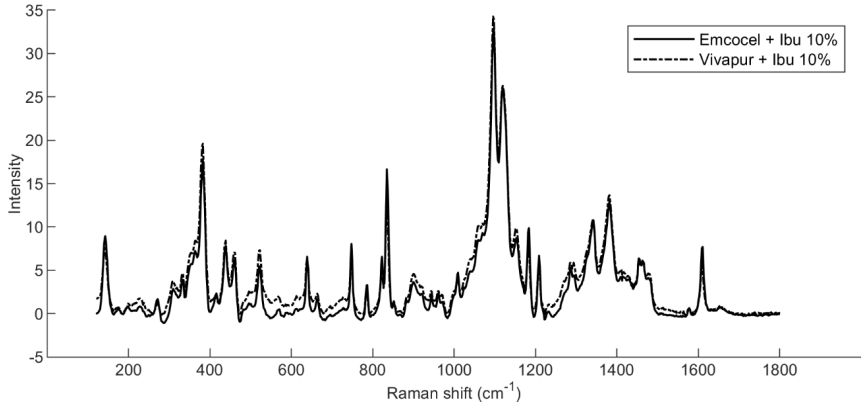
Emcocel + Ibu 10%
Vivapur + Ibu 10%
Intensity
Raman shift (cm-1)

F

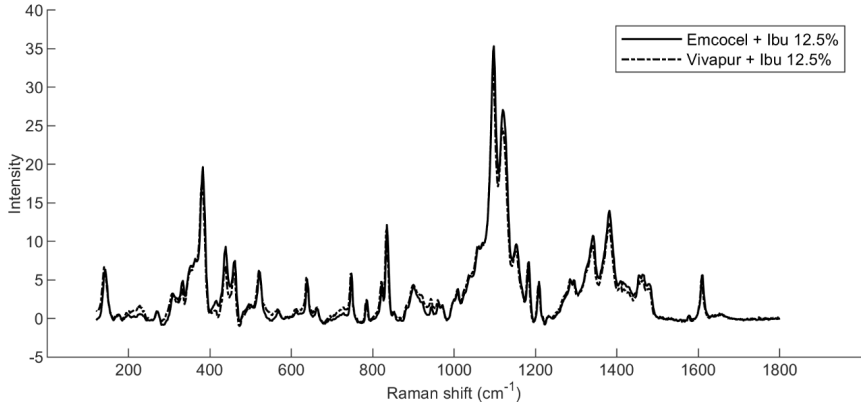
Emcocel + Ibu 12.5%
Vivapur + Ibu 12.5%
Intensity
Raman shift (cm-1)

803

G

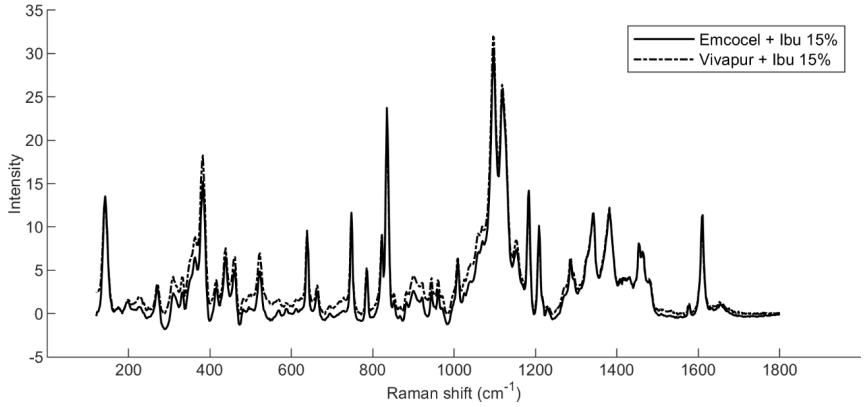
Emcocel + Ibu 15%
Vivapur + Ibu 15%
Intensity
Raman shift (cm-1)

H

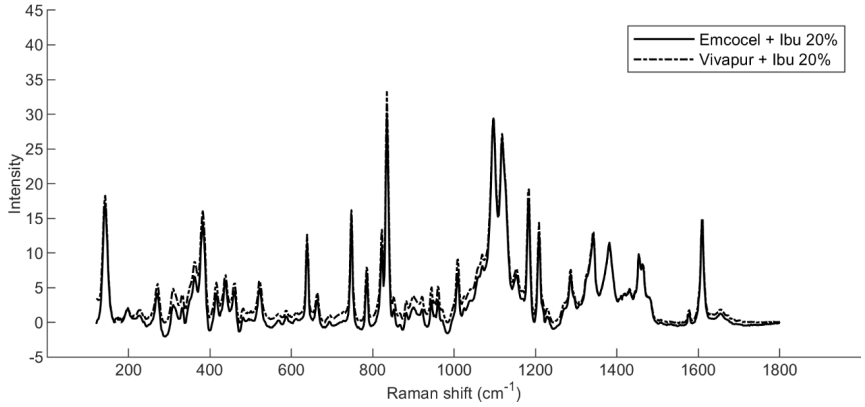
Emcocel + Ibu 20%
Vivapur + Ibu 20%
Intensity
Raman shift (cm-1)

804

I

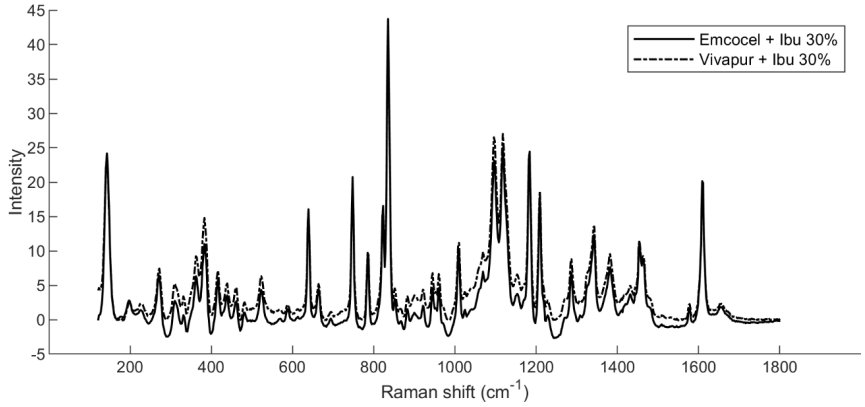

805 Figure SM-3. Raman spectra of tablet of (A) Spray dried MCC (Emcocel®) and Air stream
806 dried MCC (Vivapur®) and of the blends with ibuprofen at (B) 2.5%, (C) 5%, (D) 7.5%, (E)
807 10%, (F) 12.5%, (G) 15%, (H) 20%, (I) 30% w/w ibuprofen/MCC.

808